Comparison of ASTM Standards for the Evaluation of Geogrid Strength

Rani F. El-Hajjar, Ph.D., P.E.
Associate Professor

Hani H. Titi, Ph.D., P.E.
Professor

and

Mohammad Al-Barqawi
Ph.D. Candidate

Department of Civil and Environmental Engineering
University of Wisconsin-Milwaukee
3200 N. Cramer St.
Milwaukee, WI 53211

WisDOT ID no. WHRP 0092-19-06

February 2021

RESEARCH & LIBRARY UNIT

WISCONSIN HIGHWAY RESEARCH PROGRAM

WISCONSIN DOT
PUTTING RESEARCH TO WORK

DISCLAIMER

This research was funded through the Wisconsin Highway Research Program by the Wisconsin Department of Transportation and the Federal Highway Administration under Project 0092-19-06. The contents of this report reflect the views of the authors, who are responsible for the facts and accuracy of the data presented herein. The contents do not necessarily reflect the official views of the Wisconsin Department of Transportation or the Federal Highway Administration at the time of publication.

Technical Report Documentation Page

1. Report No.	2. Government Accession No.	3. Recipient's Catalog No.
WHRP 0092-19-06		

4. Title and Subtitle	5. Report Date
Comparison of ASTM Standards for the Evaluation of Geogrid Strength	February 2021
	6. Performing Organization Code

7. Authors	8. Performing Organization Report No.
Rani F. El-Hajjar, Hani H. Titi, and Mohammad Al-Barqawi	

9. Performing Organization Name and Address	10. Work Unit No. (TRAIS)
Department of Civil and Environmental Engineering University of Wisconsin-Milwaukee 3200 N. Cramer St. Milwaukee, WI 53211	11. Contract or Grant No. WHRP 0092-19-06

12. Sponsoring Agency Name and Address	13. Type of Report and Period Covered
Wisconsin Department of Transportation Research & Library Unit 4822 Madison Yards Way Room 911 Madison, WI 53705	Final Report November 2018 – February 2021
	14. Sponsoring Agency Code

15. Supplementary Note

16. Abstract

In this project we investigate the application of ASTM D4595, ASTM D6637 and ASTM D7737 on geogrids from more than 9 geogrid manufacturers supplying materials for Wisconsin DOT projects. The objective was to determine minimum standard guidelines that can be used in practice based on ASTM D6637 and what can be learned from the junction strength behavior in ASTM D7737. A total of 987 specimens were tested with the bulk of the testing focused on the biaxial geogrids. The objective of this research is to provide WisDOT with correlation methods for tensile strength of geogrids tested using ASTM D6637 and D4595. Evaluation of test results including the use of statistical comparison of the results and relative of the weight of the geogrids was accomplished. Recommendations on incorporating new geogrid tension strength values in WisDOT specifications are discussed.

17. Key Words	18. Distribution Statement
	No restriction. This document is available to the public through the National Technical Information Service 5285 Port Royal Road Springfield VA 22161

19. Security Classif. (of this report)	20. Security Classif. (of this page)	21. No. of Pages	22. Price
Unclassified	Unclassified		

Form DOT F 1700.7 (8-72) Reproduction of completed page authorized

Acknowledgements

This research project is financially supported by Wisconsin Highway Research Program (WHRP) and Wisconsin Department of Transportation (WisDOT).

The input and guidance of WHRP Geotechnical Oversight Committee members and WisDOT engineers Mr. Russel Frank, Mr. Robert Arndorfer, Mr. Andrew Zimmer, Mr. Zachary Gambetty, Mr. Erik Lyngdal, and Mr. David Staab, is greatly appreciated.

The research team also acknowledges the help of UW-Milwaukee student Brock Behnke.

The help and support of Dr. Mark Wayne and Ms. Lynn Cassidy of Tensar International is greatly appreciated.

Executive Summary

A geogrid is a class of geosynthetic material that is used to reinforce soils, retaining walls and other structures. In this document, we report the findings of a research program into the test methods for tension strength of geogrid materials. The geogrid materials considered are typically made of polymer materials such as polypropylene. The final shape configuration is defined by the punching pattern and extrusion parameters, in which each punch will end up as an aperture. Geogrids primarily work by tension in the ribs and junctions of the geogrid as the structure being reinforced is pulled in tension after interlocking with soil or aggregates. Given that the materials and manufacturing approaches have continuously evolved, the geogrid test methods have likewise had to adjust to changes in the materials and designs.

The Wisconsin Department of Transportation specifications have previously used the ASTM D4595 also known as the "Standard Test Method for Tensile Properties of Geotextiles by the Wide-Width Strip Method," for determining the tension properties of geogrids. The test involves testing 8-inch wide specimens of the geogrid in the machine and cross machine directions. Strength, elongation and modulus can be measured from his standard. Elongation is measured using crosshead displacement or non-contact extensometers. The gage length is typically 4 inches. A preload of 1% of the breaking force of the material is used before loading the specimen at a constant displacement rate of approximately 10mm/minute to failure. Since D4595 was originally developed for geotextiles, geogrids have unique differences in geometry which led to the ASTM D6637 standard titled, "Determining Tensile Properties of Geogrids by the Single or Multi-Rib Tensile Method," as the test method most commonly being proposed for assessment of tension properties of geogrids. The standard recognizes that the main factor involving the geogrid tension strength is the ribs per unit length of material versus simply the length. The test standard has three methods, A, B and C. Method A involves determining the tensile properties of a single rib, Method B involves a specimen with multiple ribs and Method C which involves multiple geogrid layers. Method B is the most commonly used since it is more representative of the geogrid structure and the load redistribution that may occur in the geogrid in practice. There is also another standard ASTM D7737 titled, "Standard Test Method for Individual Geogrid Junction Strength" which involves testing a single junction in isolation from the ribs. The junction or node is confined such that a single rib is pulled from the junction with the transverse rib used to obtain the maximum force or strength of the junction. Thus, it can be seen that ASTM D6637 derives the tension strength of the ribs of the geogrid whereas D7737 directly tests the junction of the geogrid. Typically, the junction strength is expected to be within a certain range of the rib strength and maybe an issue especially with the introduction of new materials.

In this project we investigated the application of ASTM D4595, ASTM D6637 and ASTM D7737 on geogrids from more than nine geogrid manufacturers supplying materials for Wisconsin DOT projects. The objective was to determine minimum standard guidelines that can be used in practice based on ASTM D6637 and what can be learned from ASTM D7737 on the geogrids used. The choice in geogrid material selection was made to mirror the types of materials, designs and suppliers used on these projects. A total of 987 specimens from biaxial, triaxial and uniaxial geogrids were tested with the bulk of the testing focused on the biaxial geogrids given they are the most common type. The results show ASTM D6637 resulting in less scatter in the tension strength compared to D4595 largely due to it more accurately capturing the mechanism of geogrid tension behavior. Variability in machine and cross-machine direction showed the importance of testing both directions. While weight of the geogrid can be correlated to the tension strength it is not recommended that the weight be used as a criterion for geogrid material selection to indicate tension strength. Uniaxial and triaxial geogrids were also tested with the standard showing the ability to meet both rib and junction strength requirements for geogrid applications. The strength derived from the 5% elongation was found to yield consistent results and also account for the material nonlinearity before rupture of the specimen. Junction strength from ASTM D7737 showed consistently favorable junction strength compared to rib tension strength from ASTM D6637 in all the test specimens examined. Recommended specifications for geogrid tension strength are provided.

Table of Contents

List of Figures

List of Tables

Chapter 1
Introduction

1.1 Problem Statement

This study focused on the geogrid tensile strength which is the one of the primary parameters used by WisDOT engineers in the design and specification of geogrids in reinforced soil structures. The Wisconsin Department of Transportation (WisDOT) currently specifies the ASTM Standard D4595 'Standard Test Method for Tensile Properties of Geotextiles by the Wide-Width Strip Method' to measure the tensile strength of geogrids. However, this specification was developed for the use on woven geotextile fabrics and not for geogrids. In recent years the geogrid manufacturers have utilized the ASTM standard D6637 'Standard Test Method for Determining Tensile Properties of Geogrids by the Single or Multi-Rib Tensile Method' in place of ASTM D4595 for determining tensile strength. The desired research outcomes would include a comprehensive study that assesses the testing mechanics, compares the results obtained with the two methods, and provides a correlation that would allow WisDOT to migrate from ASTM D4595 to ASTM D6637 in determining tensile strength of geogrids. These results are needed so WisDOT design engineers have the confidence in using the new standard for the design and specification of geogrids for the construction of earth reinforcing structures, reinforced earthen embankments and subgrade stabilization in transportation facilities.

1.2 Research Objectives

The overall objective of this research is to provide WisDOT with recommendations on geogrid tension strength values for implementation in WisDOT geogrid specifications based on ASTM D6637. This research aimed at:

i. Performing a literature search and review to document similar-type studies and ASTM documentation/history on D6637. This search will also include gathering other background data/studies that would have applicability to this research (including other state DOT's practices).
ii. Material testing of currently manufactured geogrid using both the ASTM D4595 and ASTM D6637 procedures.
iii. Evaluation of test results including the use of statistical comparison of the results.

1.3 Background

Geogrids are a subset of materials known as geosynthetic materials which are used to reinforce soils or other soft materials. They are part of a wide range of geosynthetic products that also encompass geogrids, geonets, geomembranes, geosynthetic clay liners, geofoam, geocells and geocomposites [1].

These can also be used in applications such as landfill liners, retaining walls, waterproofing of dams, and liners for reservoirs, tunnels and canals [2]. Geogrid application in WisDOT projects is primarily for pavement construction shown in Figure 1.1. Geogrids are used to reinforce retaining walls as subbases or subgrade soils below roads. Their primary benefit comes from providing tension strength in holding the soil together. Geogrids are typically manufactured from ***polymeric materials (e.g. polyester, polypropylene, polyethylene etc.).*** These materials are a common focus of the research in the Engineering Mechanics and Composites Research Lab at the University of Wisconsin-Milwaukee. They can be woven, knitted, punched and/or thermoformed from plastic sheets. The most common feature of these materials, compared with geogrids, is the wider opening (or aperture) which allows for the soil to connect from one side to the other. The load is thus carried heavily through the ribs which must provide enough strength and stiffness to transfer the loads from the horizontal to longitudinal ribs. The intersections of the horizontal and vertical ribs are typically called nodes or junctions.

The focus of this research is on the ***tensile strength of geogrids*** and on evaluating the two ASTM testing methods. Currently, WisDOT specifies the ASTM Standard D4595 'Standard Test Method for Tensile Properties of Geogrids by the Wide-Width Strip Method"[3]. However, in recent years the industry has been moving towards the ASTM standard D6637 'Standard Test Method for Determining Tensile Properties of Geogrids by the Single or Multi-Rib Tensile Method' [4].

Figure 1.1: Use of geogrid in Wisconsin pavements – STH 33 between Cashton and La Crosse, WI (Pictures by Titi, 2016)

In recent years, the large proliferation of geogrids has made it more difficult for Departments of Transportation (DOTs) to quantify geogrids and classify them. One of the challenges engineers face in using geogrids is in interpreting overlapping ASTM standards especially with respect to determining the tensile strength. The variety of fabrication methods and products make it imperative that the proper testing is deployed to check for the required properties. The current WisDOT geogrid specifications refer to ASTM D4595 for tension testing despite many industries moving to ASTM D6637. The issue is becoming more challenging for engineers, as several companies are no longer reporting the ASTM D4595 test results. The complexity of products proposed also creates new challenges in imposing the proper requirements for open area, thickness, junction efficiency and shape of the grid (Figure 1.2).

In ASTM D4595 [3], a wide specimen is gripped across its entire width in the clamps and is operated in displacement control mode increasing the force on the specimen until the specimen breaks (Figure 1.3). The tensile strength and modulus are then interpreted from the recorded data and measurements of the test specimens. Whereas the industry has been moving toward ASTM D6637 which provides more options of testing the material by providing three approaches of either testing a single representative rib specimen, a wide gripped specimen (similar to D4595) or a wide multilayered specimen. The method also provides provisions for geogrids that can slip during testing or get damaged from clamping pressure.

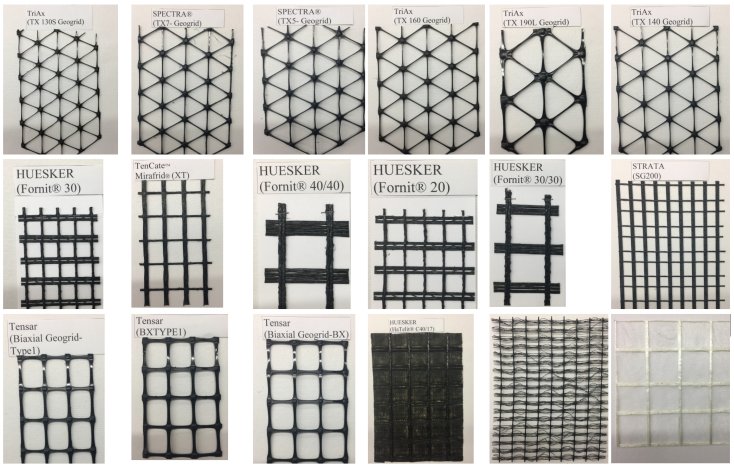

Figure 1.2: Examples of various fabrication methods used to produce different geogrids (Pictures by research team 2018).

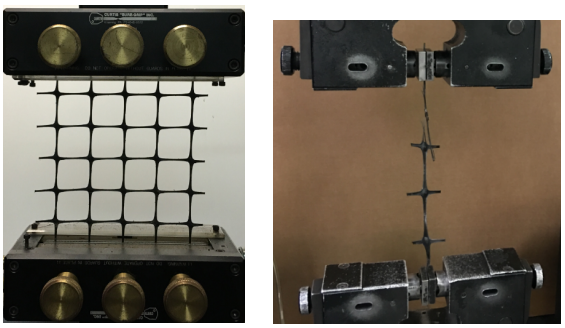

Figure 1.3: ASTM Fixtures used for Geogrid Testing (Left: wide specimen fixture, Right: Single rib fixture)

1.4 Organization of the Report

This report is organized in five chapters. Chapter One introduces the problem statement and objective of the research. The literature review is presented in Chapter Two, and the research methodology is discussed in Chapter Three. Chapter Four presents the laboratory testing program with critical analysis of the results and development of geogrid specifications. Summary, conclusions and recommendations are provided in Chapter Five.

Chapter 2
Background

This chapter presents background information on geogrid testing with emphases on tension strength using ASTM standard procedures. The focus of this research is on the tension strength of geogrids but we will discuss the characteristics and general application of geogrids before emphasis on the tension strength determination methods. The objective of this literature review is to present the current state of the literature together with a review of how various state highway agencies have addressed the specifications for geogrid tensile strengths.

2.1 Introduction

A geogrid is a class of geosynthetic material that is used to reinforce soils, retaining walls and and other structures. Geogrids are increasingly used to provide solutions when engineers encounter unfavorable soil conditions. For example, using geogrids allow a reduced thickness in a pavement structure by stiffening the sub-base. Geogrids are also increasingly the material of choice when handling failure scenarios in infrastructure retrofits by using a reduced subbase, reducing time for construction and thus overall project costs. Geogrids can be deployed to situations where there is cracking and tearing in a pavement or slope failures for more rapid repairs and resulting in thinner asphaltic top layers. According to a report by Allied Market Research, the global geogrid market generated $0.8 billion in 2018 and is expected to reach $1.8 billion by 2026. This increase is driven by the rise in infrastructure development activities across the world and a surge in adoption in the construction sector due to ease in handling, environmental safety, and high mechanical properties. The report noted that increased awareness of geogrid and an increase in research and development activities create new opportunities. The primary sector to see growth will be the road industry which represents more than one-third of the total share. Soil reinforcement is also seen as a growth area for using geogrids in road & railways, slopes & earth embankments, foundations, and retaining walls. (Khillari 2020)

The primary reinforcement occurs through a tension mechanism in the geogrid as the structure being reinforced is pulled in tension after interlocking with soil or aggregates. Geogrids are typically made from polymers with typically large apertures compared to geotextiles, another commonly used polymer material used in civil engineering applications. Geogrids are also manufactured specifically as a reinforcement material, whereas geotextiles have other functions, such as separation, drainage, and filtration. Geogrids also form a different form of reinforcement owing to the interlocking of the soil and aggregate with the grid membrane. The Geogrid material can vary between knitted or woven grids, non-woven fabrics, and composite fabrics. Geogrids are commonly made from polyester, high-density

polypropylenes, or high-density polyethylene. They are mainly fabricated using extrusion, knitting, weaving, extrusion and welding. In extruding; punched flat plastic sheets are extruded into the desired final configuration. The final shape configuration is defined by the punching pattern and extrusion parameters, in which each punch will end up as an aperture. In knitting or weaving, single yarns of polyester or polypropylene are weaved into flexible joints forming the aperture and subsequently coated with bituminous or latex coatings. In extrusion and welding, single ribs are extruded from polyester or polypropylene material and subsequently welded together into the desired shape and size. The properties of a geogrid material depend on the geometric configuration and characteristics of the materials used. The mechanical properties are influenced by the grid geometry which includes the aperture size, percent open area, and thickness. The requirements for the aperture size is that it be large enough so that aggregate and soil is able to penetrate and interlock with the geogrid. The percent open area of a geogrid is typically 50%. The grid thickness applies for both the rib and the junction thicknesses and needs to be thick enough and of adequate rigidity for soil and aggregate particles to be able to anchor against (Carrol Jr 1988) thus creating a non-uniform thickness in the geogrid with junctions typically having higher thickness values. The physical characteristics of the geogrid such as creep, tensile modulus, junction strength, and flexural rigidity are also of interest to meet the design and serviceability requirements (Whelton and Wrigley 1987, Berg and Bonaparte 1993). When loading conditions are more instantaneous, a high tensile modulus becomes more important (Institute 1987). Junction strength as a measure of the grid dimension stability and serviceability also sometimes impacts the ability of the geogrid to act as a tensile reinforcement and transfer the tension to the surrounding soil (Institute 1987). The flexural rigidity, which is the resistance of geogrid when undergoing bending, is a good indicator of the propensity of the geogrid to folding or wrinkling (Carrol Jr 1988).

2.1.1 Geogrid Physical and Geometric Characteristics

The mechanical response of geogrids is influenced by the large open space has long been considered a factor impacting the behavior of the geogrid materials. The tensile behavior of geogrids with rectangular and triangular apertures was analyzed numerically and compared to experimental results (Dong, Han et al. 2011, Qian, Han et al. 2011, Qian, Han et al. 2012, Zheng, Liu et al. 2016, Ahmadi and Moghadam 2017, Dong, Guo et al. 2018, Kim, Byun et al. 2019). Figure 2.1 shows the typical geogrids with rectangular (typically called biaxial) and triangular apertures (typically called triaxial). It was found that in biaxial aperture geogrids, the tensile strength and stiffness depend largely on the direction of the uniaxial loading relative to the orientation of the ribs. It achieved a high tensile capacity when loaded with either the machine or cross-machine direction. However, the tensile strength decreases with orienting the load away from these directions. The tensile capacity almost reaches zero at 45° load orientation. On the

other hand, the triangular aperture size geogrids carried the load uniformity at all loading directions. The compromise results in lower direction strength per material but more equally distributed. Moreover, the triangular aperture geogrids showed more uniform stress and strain distributions among its ribs compared to the rectangular aperture geogrid. It was concluded that the triangular aperture geogrid is more efficient and effective in carrying uniaxial stresses at a different orientation. The increase in the modulus of elasticity and cross-section area of ribs leads to an increase in the tensile stiffness of the triangular aperture geogrids (Dong, Han et al. 2011).

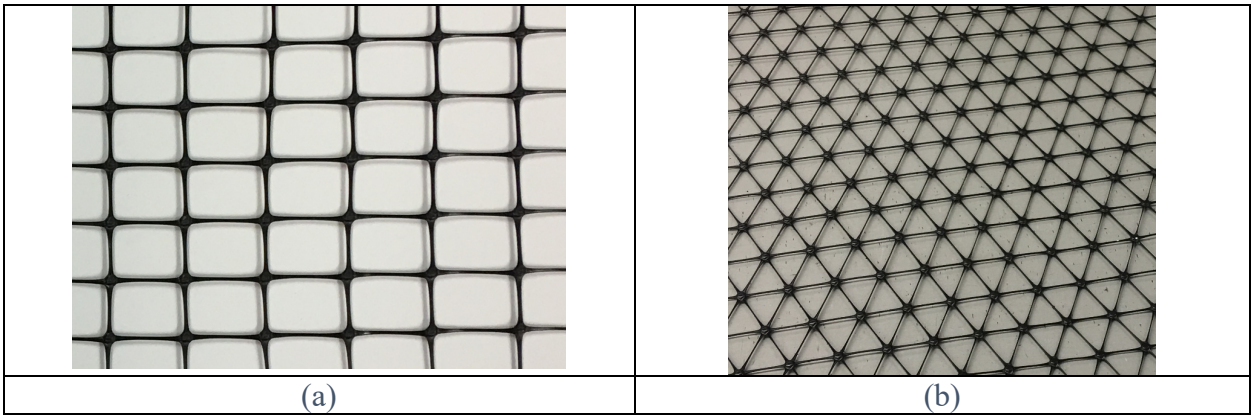

Figure 2.1 Geogrids with a) rectangular apertures and b) triangular apertures.

Geogrid samples made from high strength polyester yarn coated with PVC and cured at 180°C with five different aperture sizes were tested to determine the effect of aperture size and soil on the pullout resistance of the geogrid material (Ahmadi and Moghadam 2017). The smaller aperture size resulted in improper soil and geogrid interlock causing highly scattered results. Whereas, at a larger aperture size the frictional force between the soil and geogrid decreases. Both extreme cases resulted in a lower pull out resistance. However, the largest pull out resistance was achieved in the soil with the largest particle size. It was noticed that the pullout resistance is more sensitive to the transverse rib density of geogrids (Ahmadi and Moghadam 2017). Results show that the aperture opening showed a positive correlation with pull-out test results(Tang, Chehab et al. 2008). The maximum interaction between the geogrid and soil is achieved when the geogrid aperture size is the same or similar to that of the soil grain size (Shukla 2002). The effectiveness of some mechanical and physical properties of four biaxial geogrids (Grid A, Grid B, Grid C, and Grid D) on stabilization of pavement subgrade were studied using direct shear, pull out, and accelerated pavement tests. Grid A was made from high tenacity polyester multifilament yarns and coated with a proprietary polymer, Grid B is made of woven polypropylene yarns, Grid C is made of extruded PP Polypropylene sheets, while Grid D is made from high tenacity polyester multifilament yarns and coated with and polyvinyl chloride (Tang, Chehab et al.

2008). The study found that the most important geogrids attributes, when selecting a geogrid, were the aperture size, tensile strength at small strains, junction stress, and flexural rigidity (Tang, Chehab et al. 2008). Triaxial geogrids are increasingly popular due to the more quasi-isotropic behaviors compared to uniaxial and biaxial grids however they have not seen as much deployment in practice compared to biaxial geogrids. The triangular geogrid reinforced base course over a weak subgrade was tested against an unreinforced soil sample under cyclic loading (Qian, Han et al. 2012). It was found that the soil reinforced with triangular geogrid achieved a higher traffic benefit ratio. It was also noted that the traffic benefit ratio increased at the heavy-duty geogrid. Moreover, the maximum vertical stress and the permanent deformations in the soil decreased with the triangular geogrid reinforcement. In the reinforced sample, the stresses were more uniformly distributed among the soil and geogrid (Qian, Han et al. 2012).

2.1.2 Junctions and Connections

One of the concerns when examining the tension response of geogrid is an understanding of the load distribution between the ribs and joints in the geogrid. The junction point (also called node) in a geogrid is an important area since the stress concentrations may be amplified in this region. It is a location where there is a thickness transition compared to the ribs and where failures may initiate. In many manufacturing processes, the extrusion process, which strengthens the ribs by ordering the polymer chains, may not be at play at the junction locations. The tensile response of biaxial geogrids with integral and welded junctions under biaxial loading was experimentally investigated and test results showed an increase in geogrid stiffness when loaded biaxially “in isolation“ compared to uniaxial loading which could be related to junction response under the principal and orthogonal tensile stresses and strains due to the effect of poison’s ratio and re-orientation of the amorph molecules in the geogrid junction (Kupec and McGown 2004, Kupec, McGown et al. 2004). A similar study was conducted to evaluate the design and specifications parameters of geogrids and recommendations were presented (McGown, Kupec et al. 2005). In this study, testing techniques were presented to characterize the tensile behavior of geogrids ribs and junctions subjected to uniaxial and biaxial tensile loads. Biaxial constant rate of strain (CRS) tests showed higher stiffness than uniaxial CRS tests; however, uniaxial sustained loading tests showed higher stiffness than biaxial sustained loading tests, hence, uniaxial testing of biaxial geogrids may not completely capture the material behavior (McGown, Kupec et al. 2005). Tensile experiments have also been conducted showing that failure in geogrids in tension occurred mainly by rupture of joints and edges joining rather than the rib due to material variability in quality (Ji-ru, Lin et al. 2002). For reinforcement geogrids, the connections can be considered a limiting strength factor. Biaxial geogrids are manufactured with two-directional tensile strengths with ribs oriented in two orthogonal directions (machine and cross-machine directions) to carry the loads in both these directions and to provide more

even properties in both directions. In real applications, such as parking lots and heavy vehicle traffic conditions on construction sites, the externally applied loads may not necessarily follow the orientation of the biaxial geogrid ribs as designed, hence, it is very important to look at the biaxial geogrid response when subjected to tensile loads applied in ribs orientation in both orthogonal directions as well as tensile loads applied in directions not following the ribs orientation (Dong, Han et al. 2010). A numerical study was conducted to study the behavior of biaxial geogrids subjected to tensile loads oriented in different directions (Dong, Han et al. 2010). The geogrid was observed to exhibit both the least tensile strength and stiffness when loaded at 45 degrees angle to the machine direction due to the lower stiffness and strength in that direction as shown in Figure 2.2 (Dong, Han et al. 2010). This is to be predicted as the primary loading directions are aligned with the material axes.

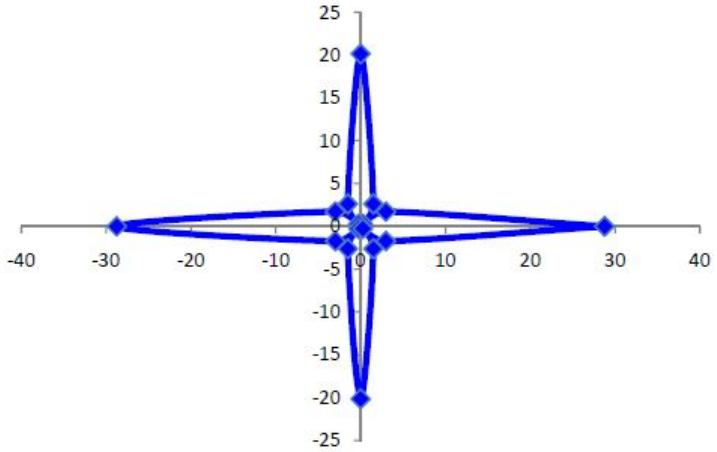

Figure 2.2: Ultimate tensile strength of tested geogrid specimens around 360 degrees loading directions (Dong, Han et al. 2010).

Another numerical investigation using finite element analysis was conducted to study the behavior of three-dimensional biaxial geogrid in piled embankment using three modeling approaches: the truss element model, the orthotropic membrane model, and the isotropic membrane model (Zhuang and Wang 2015). No significant variation was noticed between the three modeling approaches pertaining to SCR (stress concentration ratio) and subsoil settlement. Comparing the outcome of the three approaches, the orthotropic approach results were observed to be similar to the maximum geogrid strength in tension compared with the truss element approach, while the isotropic approach results were higher than the maximum tension in geogrid. Also, a parametric study has been conducted showing that increasing the pile spacing, embankment height, as well as compression index of the soil, improved the apparent geogrid tensile strength with the pile spacing having the most significant effect (Zhuang and Wang 2015) as

increasing pile spacing will result in maximum geogrid tension occurring in the pile edge rather than in the middle of pile spacing.

2.1.3 Fatigue, Creep, and Strain Rate effects

Fatigue and creep behaviors of geosynthetics are considered main design concerns for the long-term stability and serviceability of geogrid reinforced soil structures as allowable design values should not be exceeded by the long-term stresses and strains. The fatigue process in geogrids is triggered by progressively developing fissures that initiate ultimate brittle failure by reducing the intact load-bearing cross-section. The difference between maximum and minimum stresses drastically affect the fatigue strength of the material (Zanzinger, Hangen et al. 2010). In typical creep testing in laboratories, specimens are loaded to a predefined load level which is maintained constant till the end of the test and the deformation results are recorded (Kaliakin and Dechasakulsom 2001). Typically, conventional creep tests are done to evaluate the creep properties of geogrids as per ASTM D 5262. This method of testing requires a minimum time of 10,000 hours (around 1.14 years); however, this method is questionable when it comes to predicting creep behaviors of geogrids for the service life of hundred years. Other methods are used to evaluate such creep properties as discussed later in this section (Yeo and Hsuan 2010). Numerous experimental studies were conducted examining the fatigue (Nicola and Filippo 1997, Qian, Han et al. 2011, Qian, Han et al. 2012, Cardile, Moraci et al. 2016) and long term creep effects (Leshchinsky, Dechasakulsom et al. 1997, Sawicki 1998, Jeon, Kim et al. 2002, Hsieh and Tseng 2008, Hsieh 2009, Yeo and Hsuan 2010, França, Bueno et al. 2012, França, Avesani et al. 2013, Franca, Massimino et al. 2014, Bathurst and Miyata 2015) on geogrid materials. An experimental study and empirical model were developed describing the fatigue tensile behavior of uniaxially extruded geogrids made from high-density polyethylene (HDPE) considering monotonic and multistage wide-width tensile tests (Cardile, Moraci et al. 2016). The effect of varying loading parameters which include pre-stressing, frequency, amplitude, and the number of cycles on the hysteresis loops parameters which include tensile stiffnesses, maximum and accumulated residual strain for each load cycle, and area of the hysteresis loops have been explored. Results showed that increasing the number of cycles improves the hysteretic stiffness; however, it was observed to decrease when increasing the amplitude of loading. Also, a decrease in unload stiffness and an increase in reload stiffness were noticed when the number of cycles increases. Moreover, no change was noticed in the hysteretic area at lower loading amplitudes. The hysteric area increases when increasing loading amplitude at a lower number of cycles followed by a decrease for a higher number of cycles. Residual strains showed different behaviors due to loading parameter variation. It was concluded that geogrid tensile strength was not affected by the history of cyclic loading (Cardile, Moraci et al. 2016).

Polymers can be susceptible to creep effects during testing. Previous research has shown that the testing of geogrids can result in higher strengths and lower strain to failure with the speed of the test. The recommended rate of strain at 10% per minute comes from work on polyester and polypropylene fabrics which found significant effects on these properties between 1.25%/min to 12%/min (Sissons 1977). The effect of creep and stress relaxation on the behavior of HDPE and polyester geogrids has been experimentally studied (Leshchinsky, Dechasakulsom et al. 1997). Geogrids were loaded at 40, 60, and 80% of the ultimate geogrid strength for a month till creep rupture. For the case of polyester geogrids, results showed a maximum stress relaxation of 30% of the initial load, while, maximum stress relaxation of 50% of the initial load was observed for the case of HDPE geogrids. In another study, the creep behavior of both HDPE and PET geogrids using isothermal (short and long term), time-temperature superposition, and conventional methods were explored (Yeo and Hsuan 2010). It was observed that HDPE geogrid had a significantly higher creep deformation than the PET geogrid due to the polymer rubbery state which acts like a viscous fluid. Primary, secondary, and tertiary creep stages were observed in HDPE geogrids, while only primary and tertiary creep stages were noticed in PET geogrids. The creep strain rate of the primary phase was found to exponentially increase with increasing the applied load; however, the rate of the primary phase for the PET geogrid was observed to be independent of the applied load. New nonconventional equipment to conduct creep, as well as tensile tests on geogrids, was developed and presented in (Franca, Massimino et al. 2014) based on the creep testing equipment developed by Franca et al. (França, Bueno et al. 2012). The significant adjustments made to the loading system in which a rotor was placed below the equipment to prevent eccentric loading as well as reinforcing the support beam have allowed conducting tensile tests. Also, elongation measurements were taken using a new video camera approach. The tensile test results from the new unconventional equipment were in good agreement with standard tensile testing equipment results according to ASTM D6637 (ASTM 2015). However, elongation values measured at failure were much lower than the values published in the literature as the video camera approach was noticed to be more suitable for creep testing but not adequate for tensile testing; hence, enhancement for the elongation measurement system is needed. The elongation values measured by the video camera had a low coefficient of variation which proved the higher reliability of the video camera. Moreover, improvement of the loading system developed by Franca et al. (França, Avesani et al. 2013) was achieved to support higher loads which was beneficial to the tensile tests. The measured tensile strength of the geogrid in confined (within the soil) and confined accelerated conditions was observed to be higher compared with the tensile strength obtained from conventional conditions setup due to the soil geosynthetic interaction; however, the tensile strength was observed to be lower in accelerated test conditions. An experimental study was conducted to evaluate the effect of tensile strain rate on the deformation mechanism, as well as residual deformation, of

geogrids subjected to sustained and cyclic loads (Yoo, Jeon et al. 2008). Test results showed that residual deformation can be represented by the hyperbolic curve as it was observed to be significantly related to the geogrid viscous behavior. The effect of strain rate on the tensile behavior of geogrids was also studied (Hegazy, Mahmoud et al. 2018). The tests have been conducted according to ISO 10319 standard (ISO 2015) considering both single rib and wide-rib specimens at six different strain rates. The objective of the study was to come up with a valid method for single rib testing that can be closely matched with the wide-rib test without the need to conduct the wide-width test. Different strain rates have been explored and it has been observed that the geogrid tensile strength increases with increasing the strain rate for both single rib and wide width specimens. The results obtained from single rib testing using a strain rate of 100 mm/min were found to in good agreement with results obtained from the wide-width testing using a strain rate of 25 mm/min; hence, the single rib testing method was considered valid. However, it is important to consider that many specifications consider the strength at 5% strain and the correlation becomes less certain.

The impact of temperature on the tensile creep behavior of PVC coated polyester (PET) biaxial geogrids manufactured using knitting and woven techniques was experimentally studied (Hsieh and Tseng 2008). Tensile tests at various temperatures ranging from 0ºC to 80ºC were conducted according to ASTM D6637 – method A (ASTM 2015) which corresponds to single rib testing. Creep tests were conducted according to ASTM D 5262 (ASTM 2016) with 65% UTS (ultimate tensile strength) creep tensile load at various relative humidity values. Tensile test results showed a linear decrease rate (about -0.33% per ºC) in the UTS of the geogrid when temperature increases; however, the decrease rate increased slightly when going from 60 ºC to 80 ºC (Hsieh and Tseng 2008). Moreover, the elongation at break was observed to be about 11% from 0 ºC to 60 ºC and about 10.25% at 80 ºC. The reason for that is the glass transition temperature of the PET material, which is close to 80 ºC, hence, it affects the mechanical behavior of the tested geogrids at the same temperature. From the creep test results, the creep strain rate, as well as the total creep strain, were observed to increase when the temperature increases for the same loading conditions. Moreover, the creep modulus was observed to decrease when the temperature increases. It was also noticed that increasing the creep load as well as increasing the temperature reduces the rate of rupture time of the specimen. The polymer stiffness and strength can be impacted by surrounding temperature and thus the need to carefully control the environment the testing is performed. It has been shown that the tensile strength can decrease by 9.2% and 4.5% when the temperature rises from 30 degrees C to 50 degrees C with PP and PET geogrids, respectively. The elastic stiffness of the geogrid increases with an increase in the tensile load level at a fixed temperature, and decreases with an increase in the temperature at a fixed load level (Kongkitkul et al, 2012).

.

2.2 Tension Testing of Geogrids

The focus of this research is on the tension strength of geogrids. In recent years, the large proliferation of geogrids has made it more difficult for Departments of Transportation (DOTs) to quantify geogrids and classify them. One of the challenges facing engineers in using geogrids are in interpreting overlapping ASTM standards especially with respect to determining the tension strength. The variety of fabrication methods and products make it imperative that the proper testing is deployed to check for the required properties. Previous WisDOT geogrid specifications refer to ASTM D4595 for tension testing despite many industries moving to ASTM D6637. The issue is becoming more challenging for engineers, as several companies are no longer reporting the ASTM D4595 test results. The complexity of products proposed also creates new challenges in imposing the proper requirements for open area, thickness, junction efficiency and shape of the grid. Despite these similarities between D4595 and D6637 there are important differences between the two test standards. Table 2.1 shows a summary of the key differences between the two test procedures. ASTM D4595 relies on one standard specimen that can be either used with a roller or clamp type grip. However, ASTM standard D6637 has 3 types of tests to report the tension strength of the material.

Table 2.1 Summary of Key Differences between ASTM D6637 and D4595

Feature	**D4595 (ASTM)**	**D6637 (ASTM)**
Specimen Width	8 inch	Method A –Varies Method B/C – minimum value but width controlled by rib number
Specimen Gage Length	4 inch	3 junctions or 12 inches
Outer ribs treatment	None	Cut
Moisture conditioning	Yes	Yes
Multiple layers	No	Yes
Strain rate	10 ± 3 %	10 ± 3 % per minute of the gage length
Water immersion test	Yes	Yes
Clamping Restraint	Allow specimen rotation in plane	Allow specimen rotation in plane
Slack tension	Not accounted	1.25% of max or 50lb
Force	Observed force	Equivalent force per unit width and accounts for number of junctions and elements tested

Number of elements explicitly accounted for	No	Yes
Elongation accounts for slack	No	Yes
Manually applied strain	Yes	No
No. of Replicate Tests	Enough such that 95 % probability level that the test result is not more than 5.0 % of average above or below true average	Enough such that 95 % probability level that the test result is not more than 5.0 % of average above or below true average
Lab Relative Humidity	65 ± 5 %	50 – 70 %

Tension testing of geogrids presents unique problems that are not present when testing other materials. Geogrids are made of polymer materials that can experience very high elongation upwards of 20% and high mechanical loads. After the 1980s, strong geogrid type materials became more apparent which experienced difficulty when adapted to the test protocols in D4595 (Stevenson 2000) with primary issues being in gripping. Several studies have shown how gripping can significantly impact the results of testing using the D4595 method(Stevenson 2000, Hegazy, Mahmoud et al. 2018) with the rollers (capstan grips) requiring very large specimens as yielding the most consistent results. Similarly, the use of mechanical versus pneumatic or hydraulic grips can lead different results with the ability to control the grip pressure likely to lead to better results. The higher the result the more likely to approach the real strength of the material. Concern with repeatability of the testing has also been reported where it was reported that the strength and elongation from wide-width tensile tests using ASTM D4595, decrease as the number of specimen ribs increases(Hsieh and Lin 2004). The tensile strengths obtained from wide-width tensile tests were reportedly 1–8 % less than those obtained using for single rib tests. One of the differences between ASTM D-4595 and D6737 has been the details of the clamping mechanism. ASTM D-4595 provides details of wedge type clamps and roll type fixtures and criteria for rejection of grip failure. Since calculation of the load at 5% elongation, it is important to know the gage length. In this standard the gage length is measured as distance between the grips whereas ASTM D6737 more accurately defines the junction location in the grip which typically manifest itself as a protrusion within the gripping zone. In evaluating the specimen size, previous work in this area has shown the ultimate strength of the geogrid would not be impacted as much as the strain to failure. Previous work on geotextiles has shown that the woven geotextiles are most influenced by aspect ratios greater than 4 and gage lengths less than 2 inches with nonwoven geotextiles most influenced by aspect ratios less than 2 (Shrestha and Bell 1982).

The tension behavior of geogrids were studied using a video extensometer device for measuring the strains considering the effect of strain rate (Shinoda and Bathurst 2004). In this study, three types of geogrids were considered: Polyethylene terephthalate, (PET), biaxial polypropylene (PP), and uniaxial

High-density polyethylene (HDPE). The lateral strains induced in PP and HDPE geogrids were observed to be significantly larger than PET geogrid. The specimen aspect ratio was noticed to not affect the tensile response axially and laterally for the PET and HDPE geogrids, while the PP geogrid having an aspect ratio of one exhibited larger strain values than other aspect ratios. The tensile strength and stiffness of HDPE and PP geogrids were observed to increase with increasing strain rate (Shinoda and Bathurst 2004). The same conclusion on the effect of strain rate on the geogrid tensile strength and stiffness was observed in another experimental study conducted on HDPE geogrids, and it was also noticed that such effect is smaller on geogrids with high tensile strength (Yang, Pang et al. 2008). Wedge grips may not be as effective as the roller in reducing the stresses in the grips, but wedge grips have shown the ability to use them effectively to capture the properties of geogrids even in the low-strain range when using the preload method effectively.

During the testing of geogrid materials defining the point of origin in the load-displacement curve is critical because of the slack in the materials. Some materials may require some amount of preload to produce a uniform tension in the specimen and align the ribs in the specimen. In ASTM 4595 a pretension force should be provided having a minimum total applied force to the specimen of 44.5 N (10 lbf) for materials exhibiting an ultimate breaking force of 17500 N/m (100 lbf/in) and those stronger than this shall have a pretension of 1.25% of the ultimate force. The zero-position point is established from this point and used to determine the the elongation, initial modulus, and secant modulus. In ASTM D6637 the slack tension is limited to 1.25 % of the peak tensile strength or 225N (50 lbf) and calculation.

Determining the modulus from the geogrid tests can also be accomplished but is challenged by the nonlinear nature of the polymer response. It can be the most contentious to determine and specify given the dependence on the strain level it is computed for. The modulus values reported are typically secant values based on a given strain. The modulus determination is complicated by the definition of the zero-point where the test is transitioning from the slack zone to that corresponding to the active loading of the geogrid. The modulus value will be influenced by the preload value and is more impactful for lower strength geogrids. The strain level typically used for the geogrid modulus will correspond to the strain value expected during service.

2.3 Geogrid Tension Strength Specifications

Different departments of transportation have taken separate approaches to tension strength requirements in geogrids. Alabama (2018 Specifications) specifies 3 types of soil slope reinforcement with the tension strength in the machine direction from 1,000 lbs/ft (14.6 kN/m) to 3,400 lbs/ft (49.6

kN/m). Using ASTM D 5262 the strength obtained using ASTM D6637 or D4595 is reduced for creep at a 10% total strain limit. For soft soil stabilization similarly three categories are defined with requirements for both machine and cross-machine direction. The values are the same and range from 900 lbs/ft (13.1 kN/m) to 2,100 lbs/ft (30.7 kN/m). Similarly, the values for D4595 and D6637 required were the same. In Florida (2019 Standard Specifications for Road and Bridge Construction), the tension strength for machine and cross machine directions required is specified using D6637 (2%, 5%, 10% and ultimate are required depending on the application). Reinforced Soils and slopes use the 2% derived geogrid strength. In Illinois soil reinforcement and retaining walls, minimum tensile strength shall be per ASTM D6637 as specified in approved design calculations.

Table 2.2 AASHTO M288 specifications for geogrid tension testing

Test Purpose	Test Methods	Units	Requirement
Resist Installation Damage	ASTM D6637/ D6637M	kN/m	10
Ultimate tension strength based on structure specific design	ASTM D6637/ D6637M	kN/m	T_{max} x FS x RF T_{max} is determined from internal stability analysis of the wall or reinforced slope under consideration (AASHTO LRFD Bridge Design Specifications, Article 11.10.6.4.3b). FS is the safety factor, or for Load and Resistance Factor Design (LRFD), the combination of load factor divided by the resistance factor.

Georgia (2013 Standard Specifications Construction of Transportation Systems) standards for reinforced slopes the tension strengths required are based on the AASHTO Task Force 27 guidelines which use reduction factors to the ultimate strength of the geogrid for creep, site damage and durability. D4595 is used to determine the ultimate strength. A reduction factor for creep is applied based on the expected tension level at which the total strain of the geogrid is not expected to exceed 10% within the design life of 75 years. A factor is used for construction damage and in the absence of testing, a reduction factor of one-third (1/3) is applied to the ultimate tension strength of the geogrid. Evidence from manufacturer of product durability and effects on long term and short-term properties is also required. Of concern are changes in reinforcement microstructure, dimensions, mass, oxidation, environmental stress cracking, hydrolysis, temperature, plasticization, surface micrology, and variations in the infrared spectrum. In the absence of testing, a reduction factor for durability effects of one-half (1/2) is applied to the ultimate tension strength of the geogrid. West Virginia requires the ASTM D6637 with minimums on single and multi-rib results. The requirements also limit use to 25 to 30% of ultimate tension strength value based on FHWA/SA-93-025. Factors are also used for creep, installation damage and creep similar to the Georgia requirements discussed above. Delaware requirements are based on AASHTO M288 specifications for geogrid are show in Table 2.2. The ultimate strength requirement is based on structure specific design, but ASTM D6637 is used as the recommended test method. Indiana (2018 Standard

Specifications) are based on application with both tension strength and modulus are based on ASTM D6637. Junction strength is required for Type IA and IB applications. Tensile secant modulus at 5% elongation and ultimate strength for geogrids are specified per ASTM D6637. The same requirements are required for both machine and cross machine direction. The requirements are based on foundation, subgrade, embankment and modular block wall. Kentucky on the other hand (2012 Standard Specifications for Road and Bridge Construction) has specification that covers geogrid used for reinforcement of subgrade and aggregate bases. Minimum strengths are required for 2%, 5% strain and ultimate strength conditions. Junction strength at 90% of ultimate tensile strength is also required. There are also specifications for minimum and maximum opening sizes for the geogrid. Maine's requirements in (2010) Special Provision Section 620 requires reinforcement geogrid to meet ASTM D6637 tension strength at 5% elongation for both ASTM D6637. A summary of these requirements are shown in Table 2.3.

Table 2.3 Selected geogrid specifications from state departments of transportation

State	Method		Machine Direction				Cross-Machine Direction				
	ASTM D: 6637, 4595, both	Type	2% Strain (lb/ft)	5% Strain (lb/ft)	Ultimate Strength (lb/ft)	Modulus (lb/ft)	2% Strain (lb/ft)	5% Strain (lb/ft)	Ultimate Strength (lb/ft)	Modulus (lb/ft)	Comments
Alabama	Both	Soft Soil Stabilization Reinforcement Type1		500	900			500	900		
		Soft Soil Stabilization Reinforcement Type 2		800	1300			800	1300		
		Soft Soil Stabilization Reinforcement Type 3		1200	2100			1200	2100		
Florida	Both	N/A	R - 1, 3	R - 2, 3, 4, 5			R - 1, 3	R - 2, 3, 4, 5	R - 1, 2, 3, 4, 5		10% Strain is given a R - 1 through 5. R numbers are the applications the geogrid can be used for. In section 985-4.2.1 The only wording given on an exact tensile strength is, "ultimate tensile strength of all R-1 materials must be at least 4,800 pounds per foot in both MD and CMD."
Indiana	6637	Type IA & IB			800	10,000			800	10,000	
	6637	Type II				49,300					
	6637	Type III			1,500						
Maine	6637			600				1,200			
Minnesota	6637		822		2055			2055			Minnesota didn't specify what the 2,055lb/ft was defined for.
West Virgina	4595	Type I	280	580	765	15,000					
	4595	Type 2	410	810	1,080	32,000					

Chapter 3
Research Methodology

This chapter describes the laboratory testing program conducted to investigate the tensile strength of geogrid in accordance with the standard test procedures described by ASTM D4945 and ASTM D6637.

3.1 Selection of Geogrid Test Samples

The research team, in coordination with the Project Oversight Committee (POC), identified the manufacturers and suppliers of geogrid materials used in WisDOT projects. A total of 31 geogrid rolls were selected of which 987 specimens were tested as part of this project as shown in Table 3.1. From the 31 rolls selected, all were biaxial geogrid with the exception of rolls 13 and 14 which were triaxial design, and rolls 15, 16 and 17 which were uniaxial geogrid. The rolls were selected from nine geogrid manufacturers supplying geogrid materials to the Wisconsin DOT projects. The choice in geogrid material selection was made to mirror to the extent possible the types of materials, designs and suppliers.

3.2 Specimen Preparation and Quality Control

Initially, geogrid roll information is documented. This information includes roll number, manufacturer name, manufacturer product number, material type, and project number if exists. Manufacturer information is withheld due to confidentiality concerns. In addition, machine direction and cross-machine direction are labeled on the roll to avoid uncertainty. Defects and damages can be critical as they adversely affect the performance and mechanical properties of geogrids. Causes for such damages could be from manufacturing, shipment, and storage, as well as installation. A thorough inspection is conducted on geogrids to check for any defects in the roll such as punctures, tears, flaws, bent ribs, and variability in aperture sizes. Defected geogrid specimens are excluded from testing.

It is very important to measure how many ribs per unit length for the roll in both machine and cross-machine directions. This measurement is required to convert the load/rib to load/unit width as per ASTM D6637 standard. The measurement is performed by measuring a distance equals to 1-unit length (m or ft) starting at the face of one rib, then the number of ribs is counted. If the end of the 1-unit length falls inside an aperture, a fraction of the rib is included. This fraction can be calculated by dividing the distance between the face of the rib to the end of 1-unit length in the aperture by the width of the same aperture. An average of three measurements is taken in both directions. The weight per unit area of a geogrid is determined by weighing test specimens of known dimensions. A 0.5 m × 0.5 m geogrid section (measured from the center of the aperture) is weighed using a calibrated balance. The measured weight is

divided by the specimen area to get the weight per unit area for the geogrid roll. The specimens in Figure .2 are prepared as discussed below.

Table 3.1: Overview of geogrid testing program

SERIAL Number of Roll	Manufacturer	ASTM D4945		ASTM D6637 Method A		ASTM D6637 Method B		ASTM D7737	
		MD	CMD	MD	CMD	MD	CMD	MD	CMD
1	Manufacturer A	0	0	0	0	3	3	0	0
2	Manufacturer A	4	4	6	6	3	3	0	0
3	Manufacturer A	4	4	6	6	3	3	0	0
4	Manufacturer B	4	4	7	6	8	8	0	0
5	Manufacturer C	4	4	6	6	8	8	0	0
6	Manufacturer D	4	4	12	12	11	10	10	10
7	Manufacturer B	0	0	0	0	5	5	0	0
8	Manufacturer A	0	0	0	0	5	5	0	0
9	Manufacturer A	0	0	6	6	5	5	0	0
10	Manufacturer E	4	4	18	18	14	14	0	0
11	Manufacturer E	0	0	6	6	5	5	10	10
12	Manufacturer B	5	4	6	6	20	19	10	10
13	Manufacturer B	0	0	0	0	15	15	0	0
14	Manufacturer B	0	0	18	18	15	15	0	0
15	Manufacturer F	0	0	6	0	0	0	0	0
16	Manufacturer F	0	0	13	0	0	0	0	0
17	Manufacturer F	0	0	18	0	0	0	0	0
18	Manufacturer H	0	0	0	0	10	10	10	10
19	Manufacturer H	0	0	0	0	10	10	10	10
20	Manufacturer H	0	0	0	0	10	10	10	10
21	Manufacturer G	0	0	6	6	5	5	10	10
22	Manufacturer G	0	0	6	6	5	5	10	10
23	Manufacturer A	0	0	0	0	5	5	0	0
24	Manufacturer A	0	0	0	0	5	5	0	0
25	Manufacturer E	0	0	0	0	5	5	10	10
26	Manufacturer B	0	0	0	0	5	5	10	10
27	Manufacturer B	0	0	0	0	5	5	10	10
28	Manufacturer B	0	0	0	0	5	5	10	10
29	Manufacturer I	0	0	0	0	5	5	0	0
30	Manufacturer I	0	0	0	0	5	5	10	10
31	Manufacturer I	0	0	0	0	5	5	10	10
Sub-Total		29	28	140	102	205	203	140	140
Total Specimens	**987**								

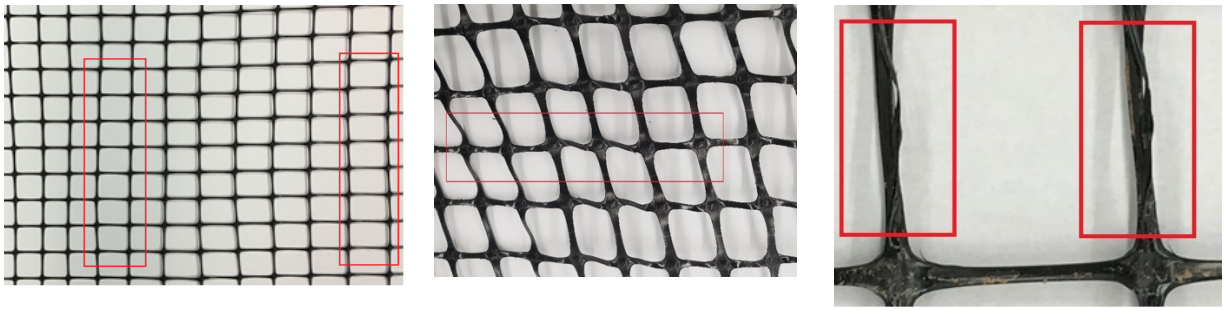

(a) (b) (c)

Figure 3.1: Manufacturing defects in geogrids, a) variability in aperture sizes, b) deformation in aperture and ribs and c) rib damage.

3.2.1 ASTM D4595 – Wide width specimen

Originally developed for geotextiles, in this test method, the specimen is prepared to be 8-inch-wide and at least 8 inches long. The length dimension of the specimen is directed parallel to the direction in which the tensile strength is measured. This method of preparation does not take into account the number of ribs being tested in the specimen.

3.2.2 ASTM D6637 – Method A (Single Rib)

This test method corresponds to single rib testing. The specimen is prepared by cutting out a single rib with a length of at least 8 inches measured from junction to junction (gage length). A total of six specimens are prepared for each testing direction (machine and cross-machine directions).

3.2.3 ASTM D6637 – Method B (Multi-Ribs)

This test method corresponds to multi-ribs testing. The specimen is prepared so that it must have a total of five parallel ribs in the direction in which the specimen is going to be tested. The specimen length should be at least 8 inches measured from junction to junction (gage length). Figure 3.2 shows a single rib and five ribs specimens. All ASTM methods call for sampling to be taken a few inches from the edges (without reference to product type) primarily because the edges are usually overlapped at the job site. However, it is important to note that the type of product can have an impact on the sampling. For example, in uniaxial geogrids the single rib tests are higher at the center and the wide width tests lower at the center. It is recommended to prepare specimens from different locations in the geogrid roll to account for material variability. Figure 3.3:shows the extent of this variability and importance of proper sampling in the roll even using the new standard D6637 Method B. Figure 3.4 depicts picture of biaxial and triaxial geogrid with illustration of geogrid orientation for machine direction (MD) and cross machine direction (CMD, sometime referred to as XMD).

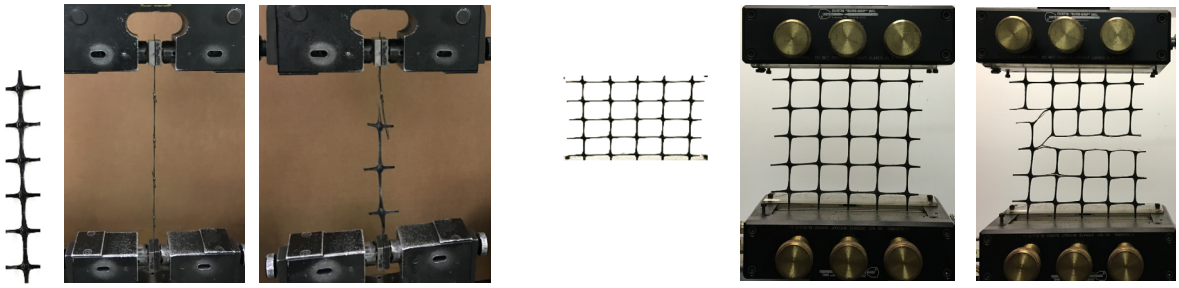

Figure 3.2: Single rib and Multi-rib specimens for Methods A and B, respectively of ASTM D6637.

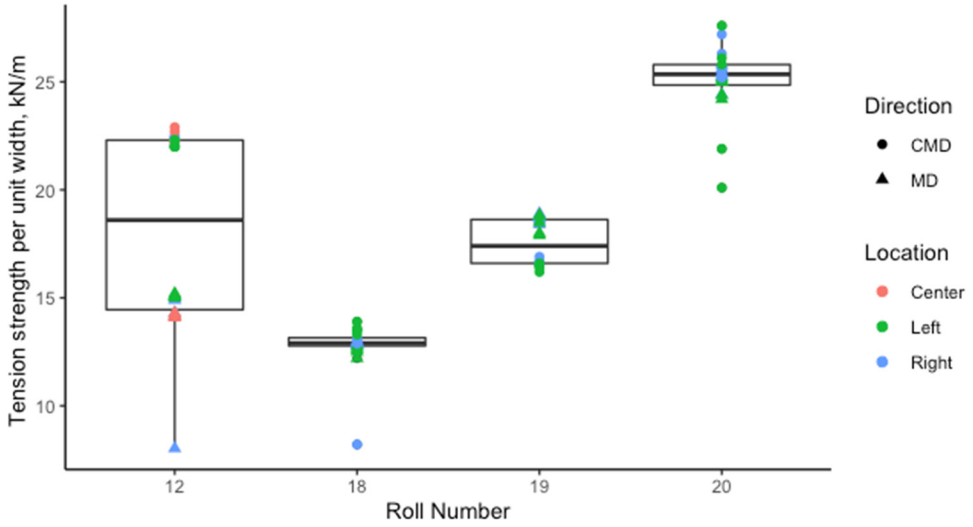

Figure 3.3: Variability of tension strength in geogrid based on sampling locations (results also show large differences between machine direction and cross-machine direction strengths). Tension strength determined from D6637 Method B with load at 5% elongation.

3.3 Methods

3.3.1 ASTM D6637 Tensile Properties using Single and Multi-rib Methods

The specimen is clamped by mounting top and bottom junctions at the centerline of each grip. The grips are adequately tightened so that to avoid specimen slippage or specimen damage which can cause premature failure. The gage length is the distance between the clamped junctions. A pretension load is applied to eliminate any slag in the material. After zeroing out the displacement, the tensile load is applied using a constant strain rate ranging from 7-13% of the gage length per minute until the specimen ruptures. Figure 3.5 shows biaxial geogrid specimen before and after testing using D6637 Method B.

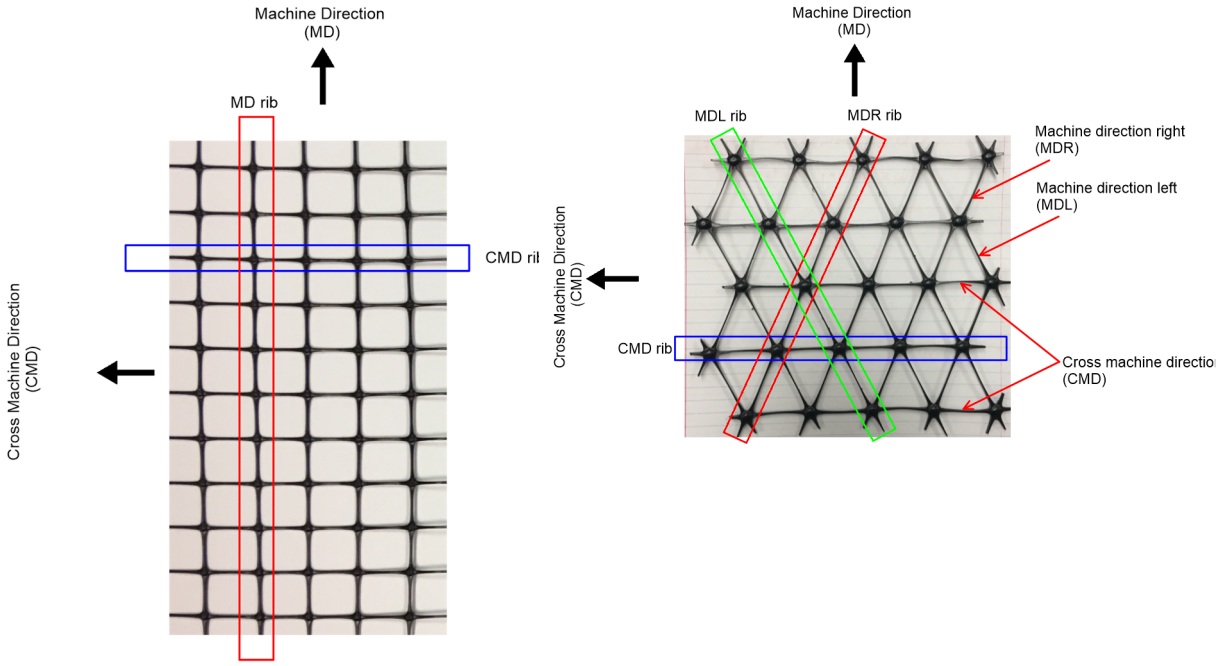

(a) Biaxial geogrid (b) Triaxial geogrid

Figure 3.4: Geogrid orientation

ASTM D6637 – Method A (single rib): A single rib is clamped properly by mounting top and bottom junctions at the centerline of each grip. Tensile load is applied at a prescribed fixed strain rate until the specimen ruptures. The ultimate tensile load for the single rib is determined based on the average of six single rib tensile tests.

ASTM D6637 – Method B (multi ribs): Wide specimen is clamped properly by mounting top and bottom junctions (total of five junctions on each side) at the centerline of each grip. Tensile load is applied at a prescribed fixed strain rate until the specimen ruptures. The ultimate tensile load per unit length is determined by the following equation:

$$\alpha_f = \frac{[(F_p - T_o)]}{N_r} N_t \qquad \textbf{Equation (3.1)}$$

Where α_f is the ultimate equivalent for load per unit width, F_p is the maximum load or load at 5% elongation, T_o is the slack tensile load, N_r is the number of ribs tested in the testing direction (typically equals 5 for method B), N_t is the number of ribs per unit length of the roll in the cross-testing direction

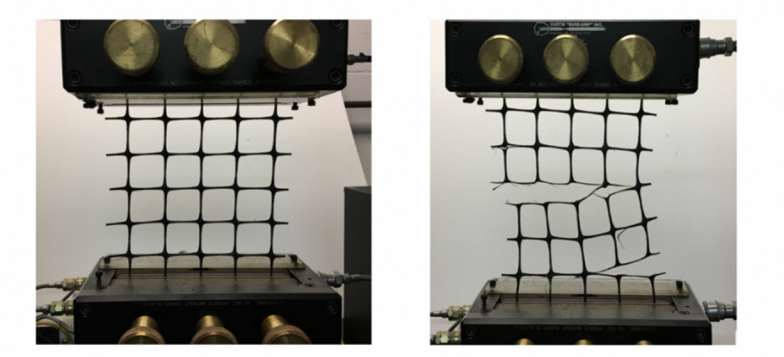

Figure 3.5: Geogrid specimen before and after testing using D6637 Method B.

3.3.2 ASTM D7737 Junction Strength

In this part of the test program, testing of an individual geogrid junction (or node) was performed per ASTM D7737 [50]. The test consists of a single rib pulled from its junctions with the transverse rib to the test direction used to obtain the strength of the junction. The value of the junction strength can be used to understand the quality of the junction relative to the ribs and the extent of handling damage that may have occurred to the geogrid. The junction or node is confined such that a single rib is pulled from the junction with the transverse rib used to obtain the maximum force or strength of the junction. Fourteen rolls were selected from the main test program and junction testing was performed for comparison to the rib strength obtained from ASTM D6637 Method B [42]. For each roll, 10 specimens were tested in the machine direction and 10 specimens in the cross-machine direction respectively. Sampling, grip details and representative fractured specimen is shown in Figure 3.6. The test specimen was loaded at a rate of 50 mm/min at room temperature conditions. A total of 280 junction specimens were tested.

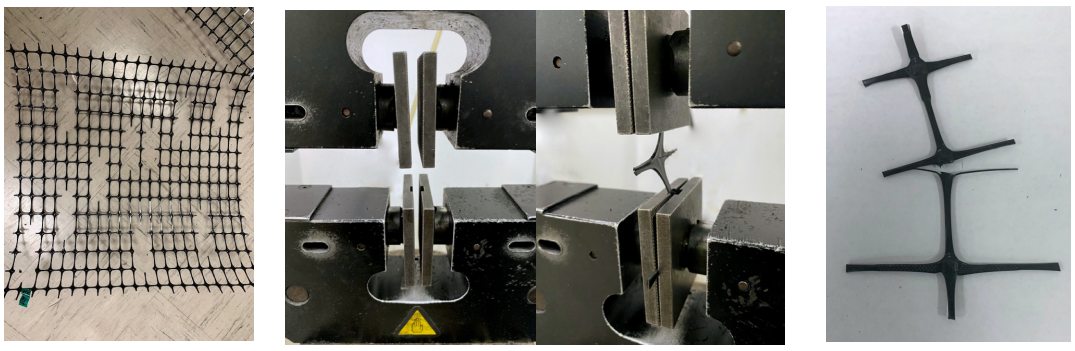

Sampling for test specimen

D7737 grips and specimen in jaws

Test specimen at break

Figure 3.6: Material preparation and testing for junction strength testing using ASTM D7737.

Chapter 4
Laboratory Tests on Geogrid Samples – Results and Analysis

This chapter presents the results of the laboratory testing program on the geogrid specimens tested using both ASTM D4595 and D6637standard procedures. Laboratory test results are analyzed and evaluated.

4.1 Geogrid Tension Test Results

Figure 4.1 depicts typical relationship between tension load (or force in pounds) versus extension (in inches) of biaxial geogrid specimens using ASTM D4595 and ASTM D6637(both method A of single rib and method B of multiple ribs) standard test procedures. The results are presented for geogrid specimens tested in both machine and cross machine directions. In addition, results of tension load (lb) and load per unit width of geogrid (lb/ft) at 2% strain (elongation), at 5% strain, and at failure (ultimate) are presented in tables inserted within each figure. The results in Figure 4.1 are for biaxial geogrid specimens of two different grades used by contractors in WisDOT projects and from the same manufacturer (Figures 4.1e and 4.1f are for a different grade geogrid). ASTM D6637Method A test results are reported only in load in pounds as described by the standard test procedure. Inspection of the plots of Figure 4.1 shows consistency in the load-extension behavior and repeatability of test results among the tested specimens in each category (i.e. ASTM D4595, ASTM D6637A&B, MD, and CMD).

In order to evaluate the variability of the results, tension tests were conducted on 188 specimens from three rolls of biaxial geogrid using the standard procedures ASTM D4595 and ASTM D6637Methods A and B. The three biaxial geogrid rolls (serial numbers (SN) 23, 24 and 12) have been widely used by contractors in WisDOT projects and represent a typical biaxial geogrid used for subgrade improvement/stabilization and base reinforcement. As shown in Figure 4.2 for roll SN23, the tension strength at 5% strain (elongation) varies between 485 and 754 lb/ft with an average of 586 lb/ft and COV of 22% when ASTM D4595 procedure is used to test specimens in machine direction. The test results using ASTM D6637Method A range from 608 to 763 lb/ft with an average of 649 lb/ft and COV of 7%. It should be noted that ASTM D6637Method A reports the results in load pound not in lb/ft; however, the roll characteristics as described by ASTM D6637Method B were used to calculate the results in lb/ft only for the sake of comparison with the results from ASTM D4595 and ASTM D6637B. The tension strength varies between 588 and 768 lb/ft with an average of 629 lb/ft and COV of 8% when ASTM D6637B method was used. These results are, in general, more consistent and repeatable when ASTM D6637test procedure are used compared with ASTM D4595. The results for roll SN24 and SN12 are presented in Figures 4.3 and 4.4, respectively, and the values/ranges/COVs are summarized in Tables 4.1 to 4.3.

(a) ASTM D4595 Machine Direction

(b) ASTM D4595 Cross Machine Direction

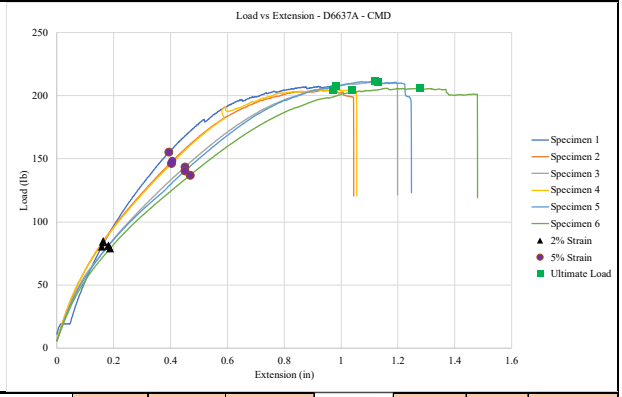

	2% Strain Load (lb)	5% Strain Load (lb)	Ultimate Load Load (lb)		2% Strain Load (lb)	5% Strain Load (lb)	Ultimate Load Load (lb)
Specimen 1	73	134	186	Specimen 4	67	120	187
Specimen 2	71	121	182	Specimen 5	70	122	189
Specimen 3	72	122	185	Specimen 6	67	122	184

(c) ASTM D6637Method A Machine Direction

	2% Strain Load (lb)	5% Strain Load (lb)	Ultimate Load Load (lb)		2% Strain Load (lb)	5% Strain Load (lb)	Ultimate Load Load (lb)
Specimen 1	81	155	208	Specimen 4	84	146	205
Specimen 2	85	148	204	Specimen 5	81	141	212
Specimen 3	81	144	211	Specimen 6	79	137	206

(d) ASTM D6637Method A Cross Machine Direction

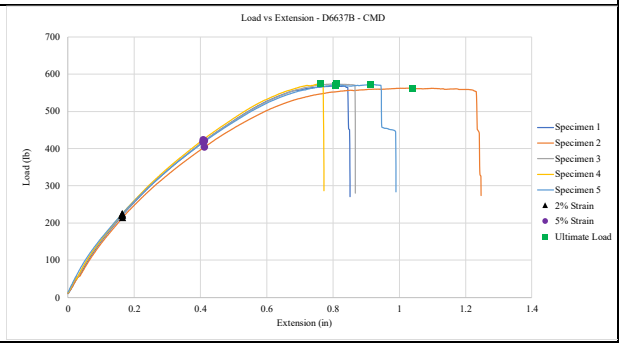

(e) ASTM D6637Method B Machine Direction

(f) ASTM D6637Method B Cross Machine Direction

Figure 4.1: Typical plots of tension load versus extension of biaxial geogrid specimens using ASTM D4595 and ASTM D6637including tabulated results of load and load per unit width of geogrid at 2% strain, 5% strain, and failure (ultimate).

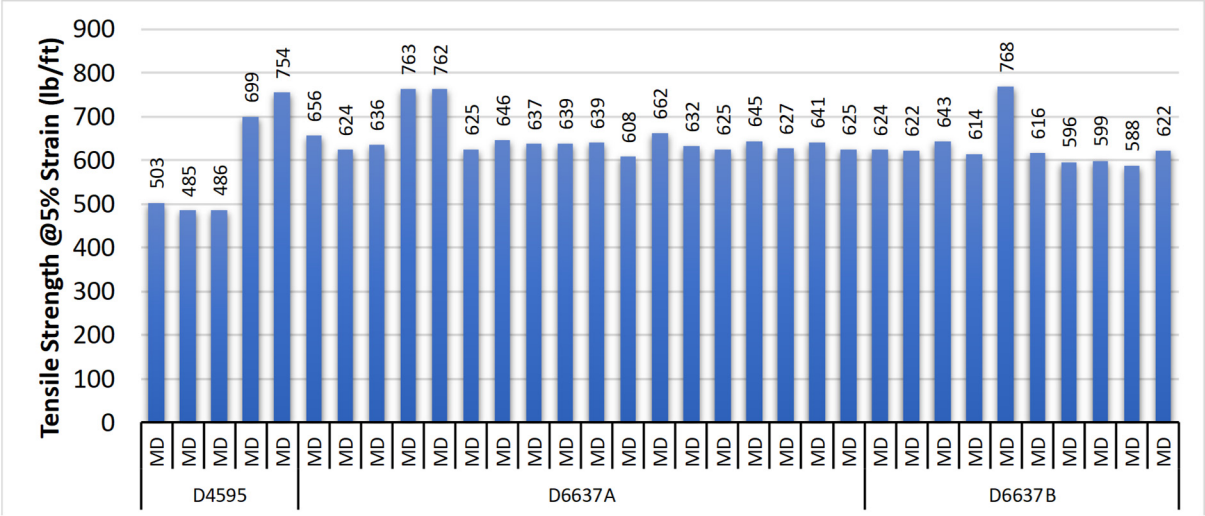

(a) Geogrid tested along machine direction

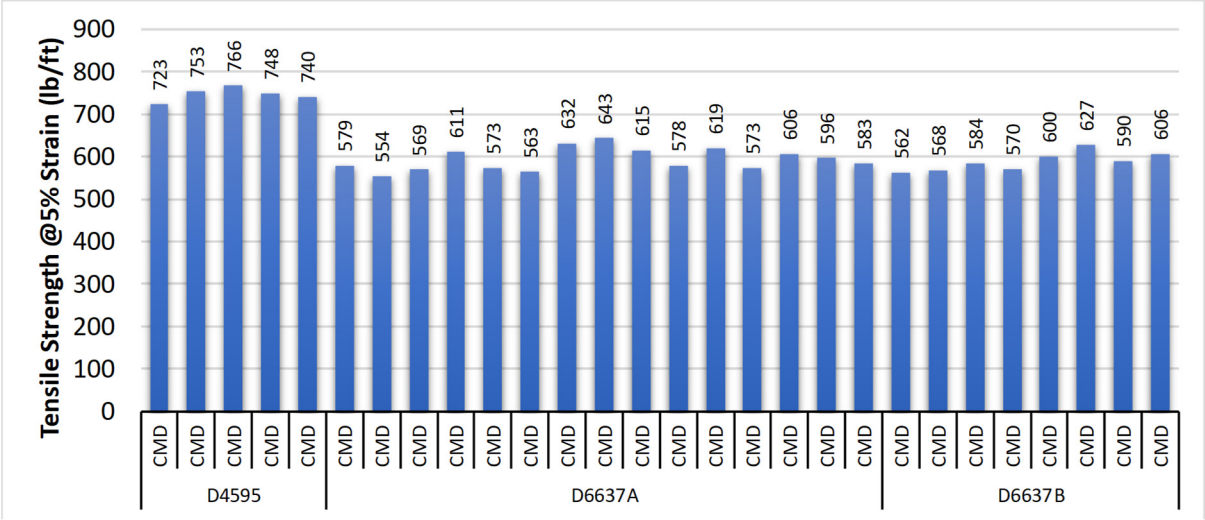

(b) Geogrid tested cross machine direction

Figure 4.2: Tensile strength @ 5% strain (using ASTM D4595 and D6637 A & B) for biaxial geogrid specimens from roll SN23.

Table 1: Statistical parameters for roll SN23

ASTM Test	Direction	Tensile Strength @ 5% Stain (lb/ft)				COV (%)
		Maximum	Minimum	Average	Standard Deviation	
D4595 (Old)	MD	754	485	586	131	22
D6637A (Single Rib – New)	MD	763	608	649	43	7
D6637B (Multiple Rib – New)	MD	768	588	629	51	8
D4595 (Old)	CMD	766	723	746	16	2
D6637A (Single Rib – New)	CMD	643	554	593	27	4
D6637B (Multiple Rib – New)	CMD	627	562	588	22	4

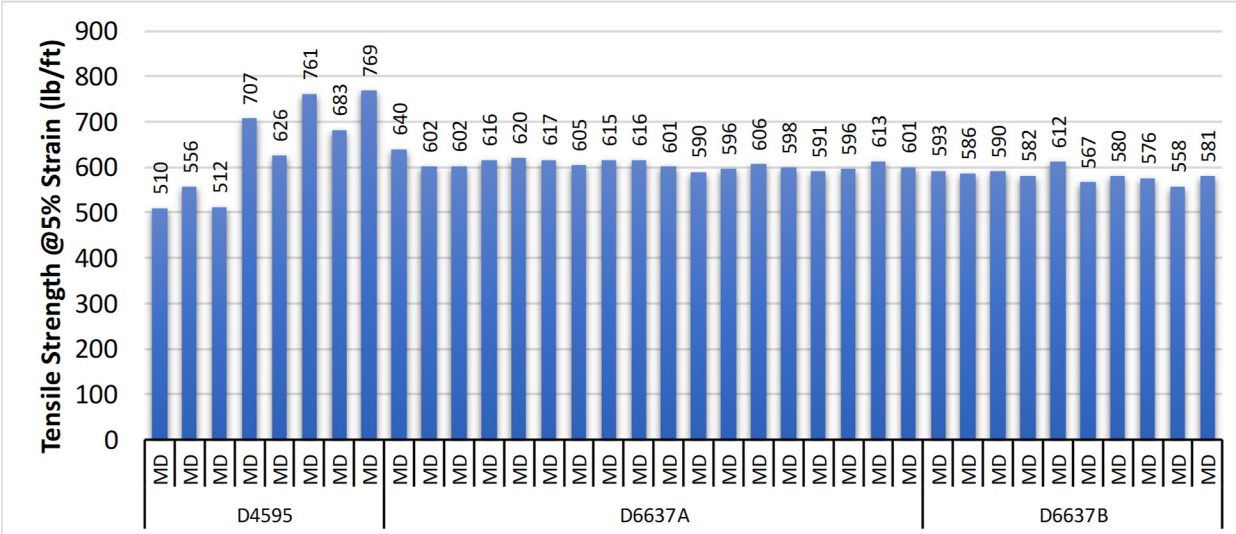

(a) Geogrid tested machine direction

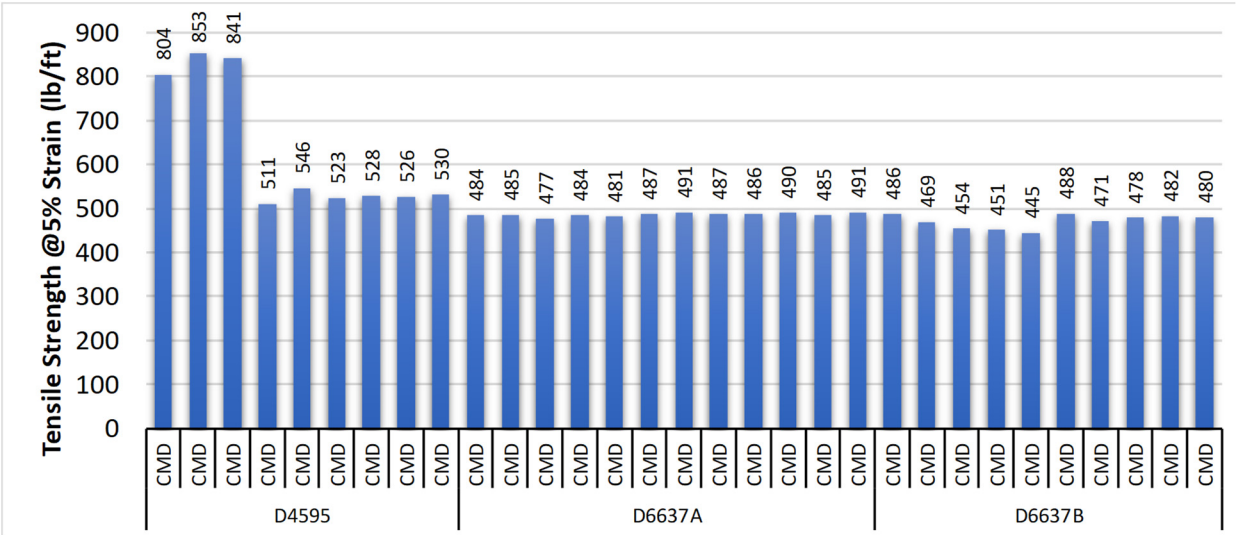

(b) Geogrid tested cross machine direction

Figure 4.3: Tensile strength @ 5% strain (using ASTM D4595 and D6637 A & B) for biaxial geogrid specimens from roll SN24.

Table 4.2: Statistical parameters for roll SN24

ASTM Test	Direction	Tensile Strength @ 5% Stain (lb/ft)				COV (%)
		Maximum	Minimum	Average	Standard Deviation	
D4595 (Old)	MD	769	510	640	105	16
D6637A (Single Rib – New)	MD	640	590	607	12	2
D6637B (Multiple Rib – New)	MD	612	558	582	15	3
D4595 (Old)	CMD	853	511	629	153	24
D6637A (Single Rib – New)	CMD	491	477	486*	4	1
D6637 B (Multiple Rib – New)	CMD	488	445	470*	16	3

* Geogrid roll has significant variability in rib length, rib thickness, aperture dimensions (see Figure 4.4)

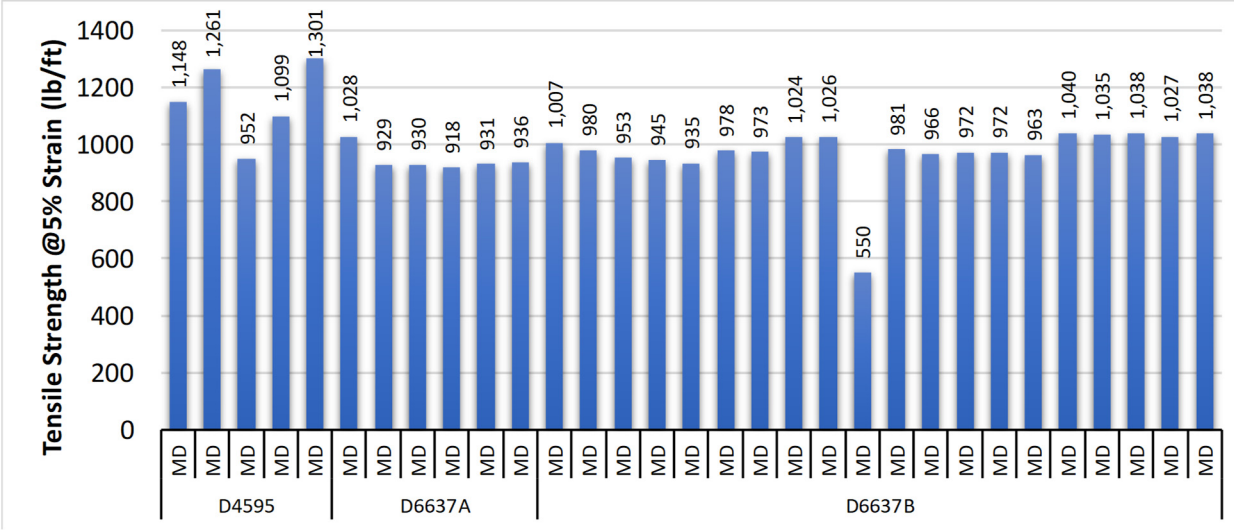

(a) Geogrid tested along machine direction

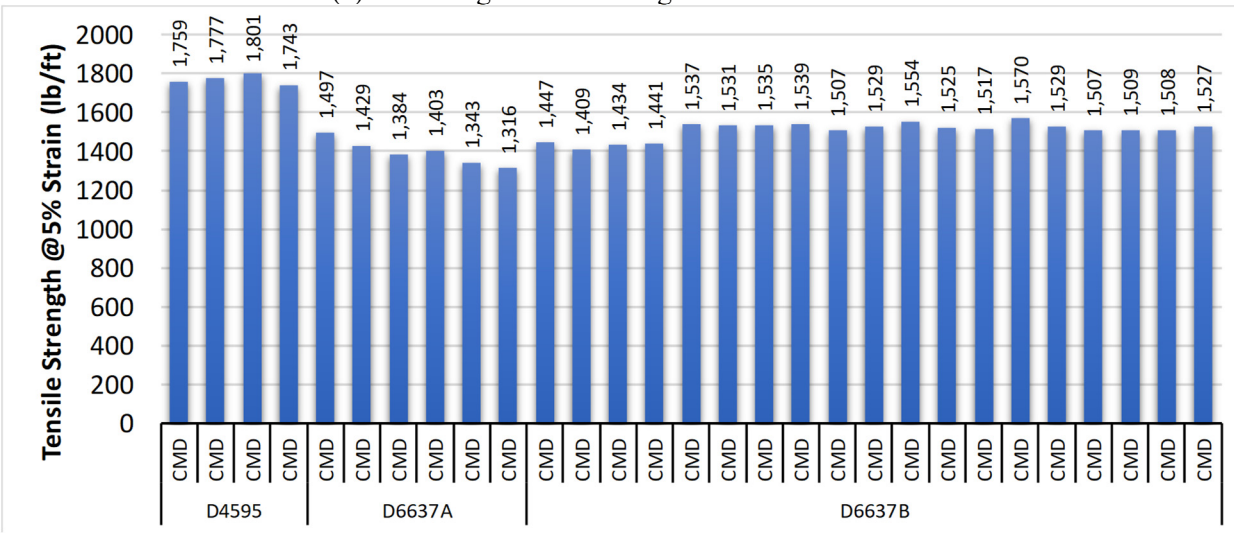

(b) Geogrid tested cross machine direction

Figure 4.4: Tensile strength @ 5% strain (using ASTM D4595 and D6637 A & B) for biaxial geogrid specimens from roll SN12.

Table 3: Statistical parameters for roll SN12

ASTM	Direction	Tensile Strength @ 5% Stain (lb/ft)				COV (%)
		Maximum	Minimum	Average	Standard Deviation	
D4595 (Old)	MD	1,301	952	1,152	139	12
D6637A (Single Rib – New)	MD	1,028	918	945	41	4
D6637B (Multiple Rib – New)	MD	1,040	550	970	104	11
D4595 (Old)	CMD	1,801	1,743	1,770	25	1
D6637A (Single Rib – New)	CMD	1,497	1,316	1,395	64	5
D6637B (Multiple Rib – New)	CMD	1,570	1,409	1,508	44	3

While the test results showed consistency and repeatability within the same standard test procedure, there were differences in the results when different test procedures are used. The main reason attributed to the difference is the characteristics of the geogrids roll and quality of the product in terms consistent aperture dimensions and rib thickness. For example, roll SN24 test results in cross machine direction using ASTM D 6637, methods A and B showed lower than expected tension strength per unit width of geogrid, which is attributed to variability in geogrid characteristics as depicted in Figure 4.5.

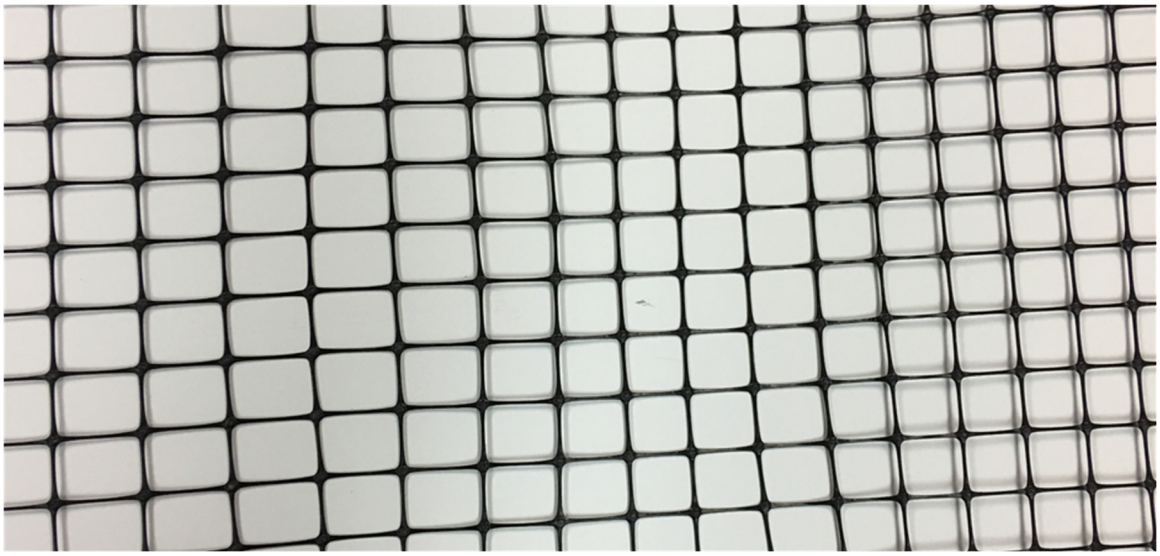

(a) Distortion in grid

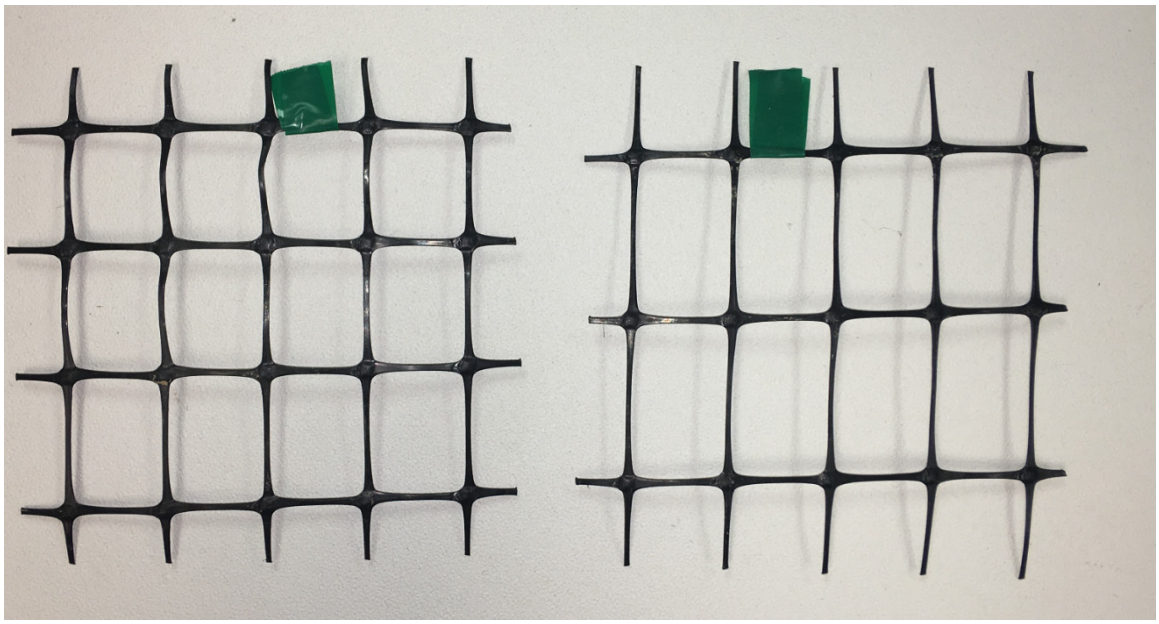

(b) Roll SN23

Figure 4.5: Significant variability in aperture dimensions and rib thicknesses observed in geogrid materials provided for possible use in WisDOT projects.

4.2 Comparison of ASTM D4595 and ASTM D6637

The results presented earlier are a select subset focused on the biaxial geogrid commonly used by contractors in WisDOT projects for subgrade improvement/stabilization and base reinforcement. Figure 4.6 depicts the use of biaxial geogrid for such applications on STH 33 near Middle Ridge, Wisconsin.

Figure 4.6: Use of biaxial geogrid for subgrade improvement/stabilization and base reinforcement in Wisconsin (Pictures by Titi, 2016).

While the focus of this study was on the biaxial geogrid, the uniaxial and triaxial types of geogrid are also investigated in this research. Figure 4.7 present the results of tests conducted in this study including the following variables: geogrid type (uniaxial, biaxial, triaxial), tension test procedure (ASTM D4595 and ASTM D6637A & B), and geogrid orientation (machine and cross machine directions). Figure 4.7 depicts Box-Whisker plot of all tension tests conducted showing the minimum, maximum, median, and upper and lower quartiles. The outliers are not shown in these plots. Results from ASTM D6637Method B and ASTM D4595 across the different weights show less scatter in the values for the tension strength per unit width from ASTM D6637than the ASTM D4595 method (Figure 4.8). Note that the results for the tension strength are based on the 5% elongation results. This may be attributed to more accurate assessment of the tension strength in the ASTM D6637standard accounting for the number of ribs and not simply the width of the specimen. Inspection of Figure 4.8 shows the higher variation in test results when using ASTM D4595 procedure compared with the test results from both Methods A and B in ASTM D 6637. Variability studies were focused on a subset of the data where we had both ASTM D4595 and D6637 specimens and mainly in the range of 4 to 6 oz/yd2. It is from those tests we can see reduced deviation when using ASTM D6637 methods. Note that the variability appears to increase in the ASTM D6637results for both Methods for the higher strength geogrid materials, but ASTM D4595 constitute only a small subset of the test database beyond 6 oz/yd^2 so this variability is likely related to roll or material variability. In general, the average tension strength from the cross-machine direction exceeds the results from the machine direction for all test types. The single rib test, Method A in ASTM D6637does show a correlation to Method B, but the variability is not consistent across the entire weight range.

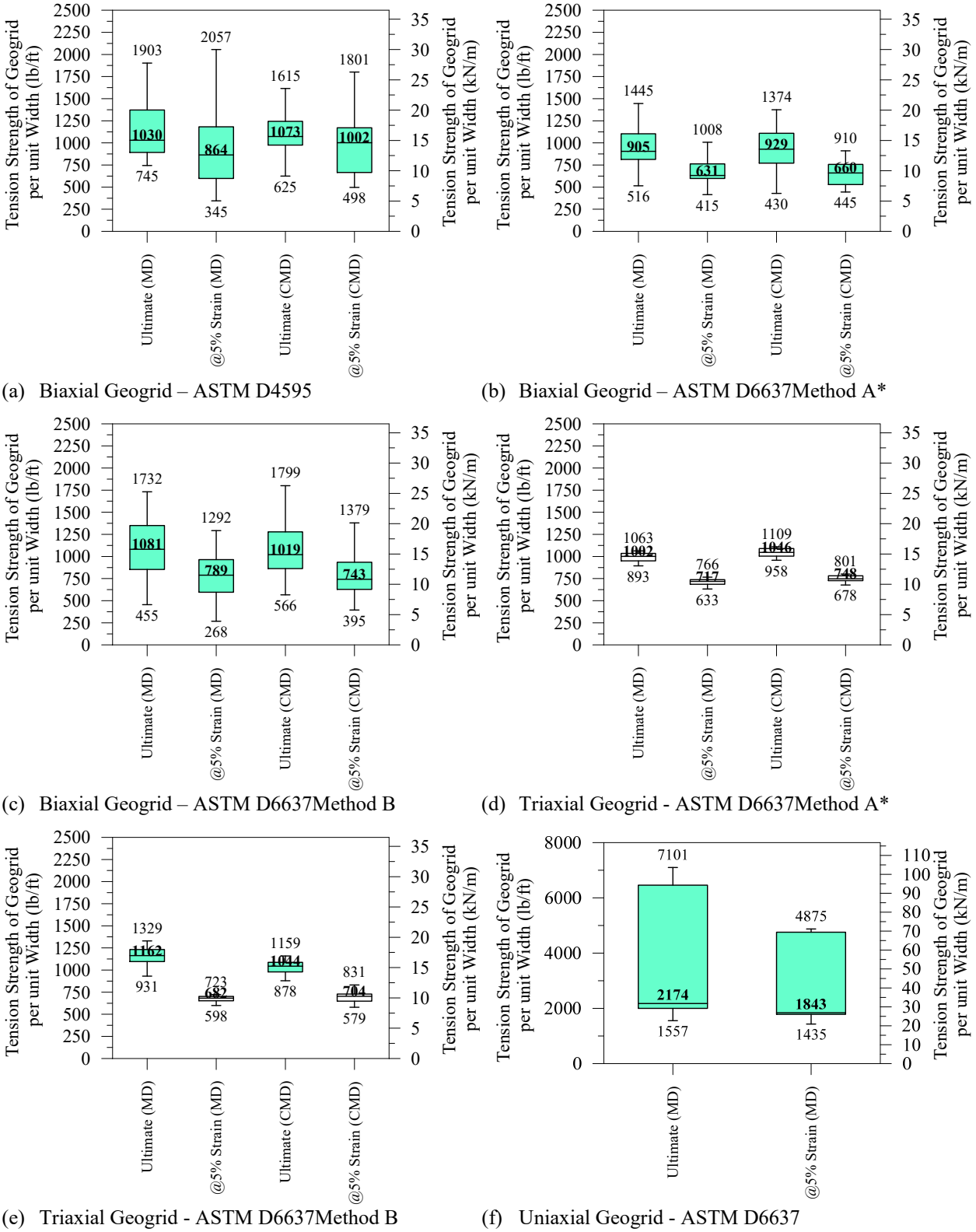

(a) Biaxial Geogrid – ASTM D4595

(b) Biaxial Geogrid – ASTM D6637Method A*

(c) Biaxial Geogrid – ASTM D6637Method B

(d) Triaxial Geogrid - ASTM D6637Method A*

(e) Triaxial Geogrid - ASTM D6637Method B

(f) Uniaxial Geogrid - ASTM D6637

Figure 4.7: Box-Whisker plot of tension strength tests conducted in this study

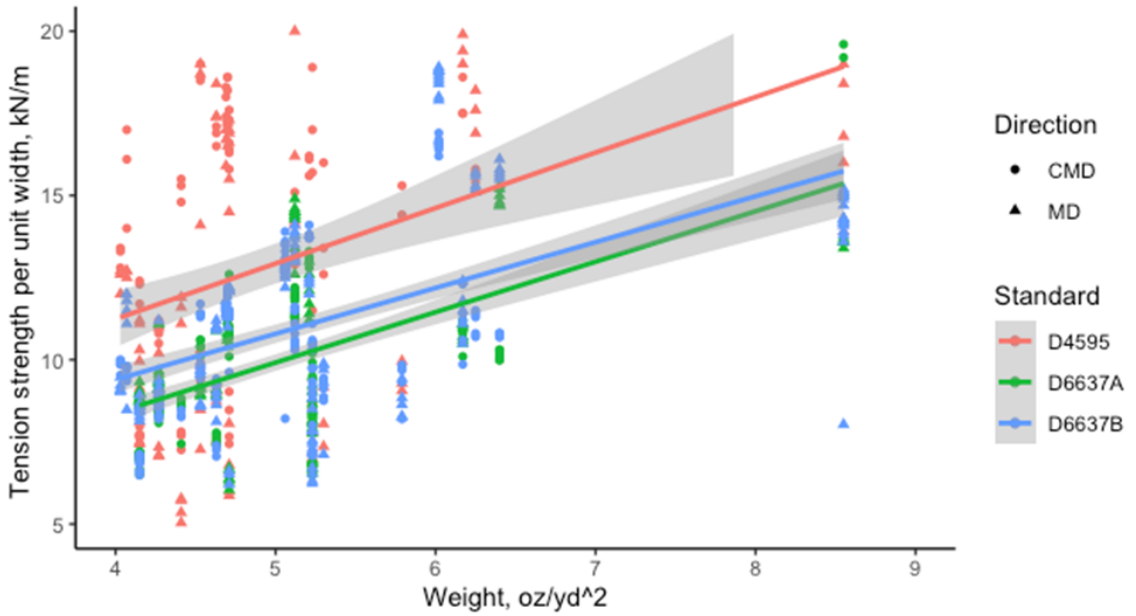

Figure 4.8: Tension strength per unit width at 5% elongation versus weight of geogrid roll tested (results from ASTM D6637 Method A adjusted by average number of ribs per unit width in the roll).

4.3 Junction versus Rib Strength

Junction efficiency (%) is evaluated as the ratio of the ultimate load junction strength to the rib strength. The average junction strength per unit width is calculated as the product of the average junction strength pre rib and the number of tensile elements in the testing direction per unit width. A Pearson correlation was performed on the results from the junction and rib derived tension strengths. The correlation test is used to evaluate the association between the two variables. A p-value of the test was obtained at 2.2×10^{-16}, which is less than the significance level alpha $\alpha = 0.05$. We can conclude a strong correlation with a correlation coefficient of 0.97 and a p-value of at 2.2×10^{-16}. Figure 4.9 shows the tension strength derived between the junction strength and the rib strength with the Pearson correlation shown in the figure. A linear relation is observed for most of the data range. Figure 4.9 also shows high junction efficiency for the specimens based on the ultimate load values. Most tested geogrid specimens had a junction efficiency greater than 100% indicating the rib strength from ASTM D6637 is adequate for characterization of the geogrid materials. The results show a consistency in this behavior across the materials from the different vendors selected as seen in Figure 4.10. The joint strength is higher than the rib strength.

Figure 4.11 depicts pictures of biaxial geogrid failure modes during the tension tests. Majority of breakage observed occurred in the geogrid ribs. While ribs failed along the breakage line, other ribs showed a fibrillating behavior. In addition, some geogrid specimens failed on the junction as well as along the junction and ribs together.

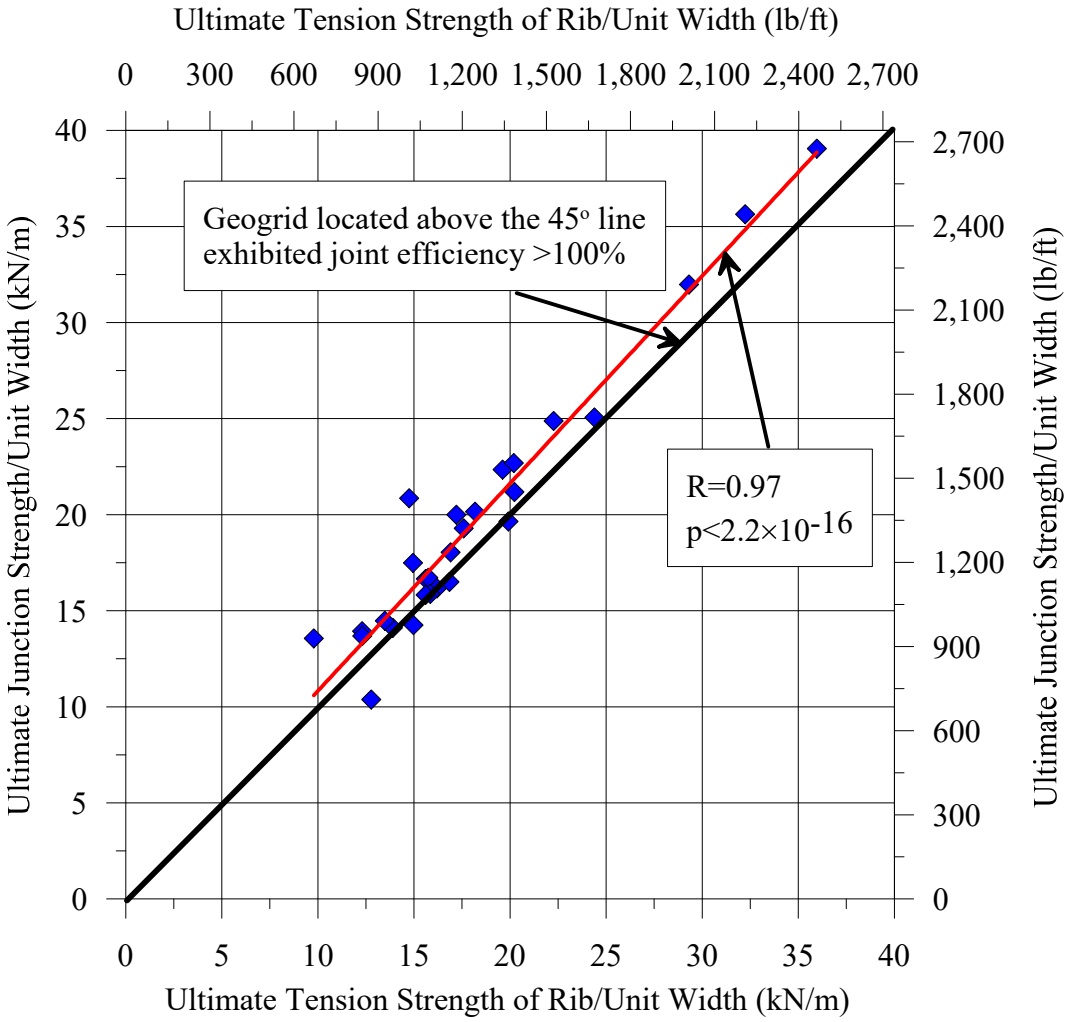

Figure 4.9: Average junction versus rib strength per unit width obtained from ASTM D7737 and ASTM D6637(each data point on the figure represents the average of 5 tests from ASTM D6637Method B corresponding to average rib strength and 10 specimens from ASTM D7737 corresponding to average junction strength. Figure includes data from MD and CMD directions and data from 14 different rolls across 6 different vendors. Rib strength based on ultimate force.

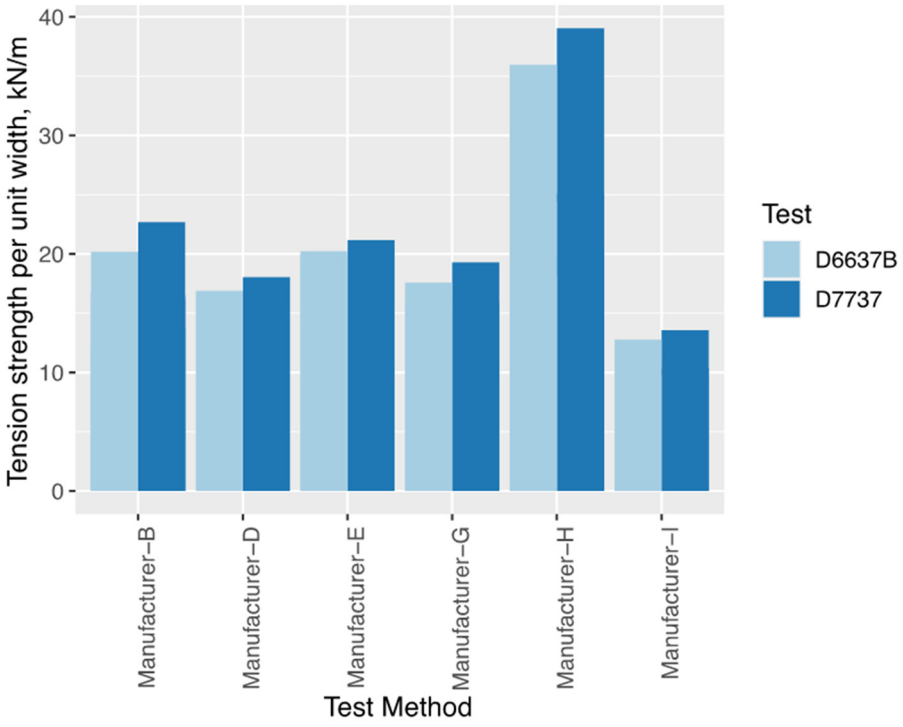

(a) Machine direction

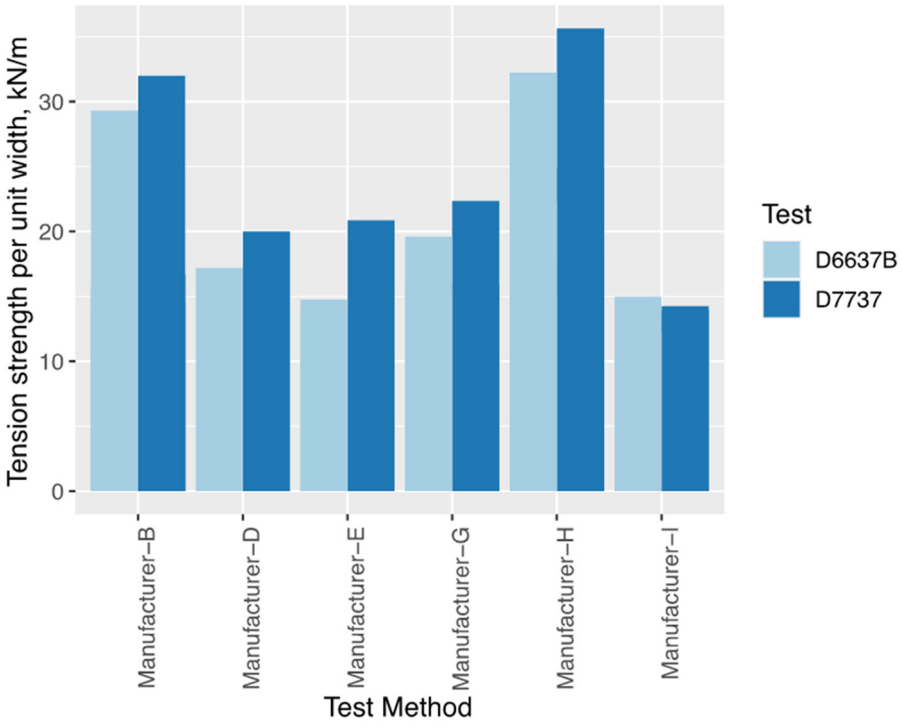

(b) Cross Machine direction

Figure 4.10: Comparison of junction and rib tension strength per unit width across various biaxial geogrids showing junction strength from ASTM D7737 is typically higher than rib derived strength in ASTM D6637Method B.

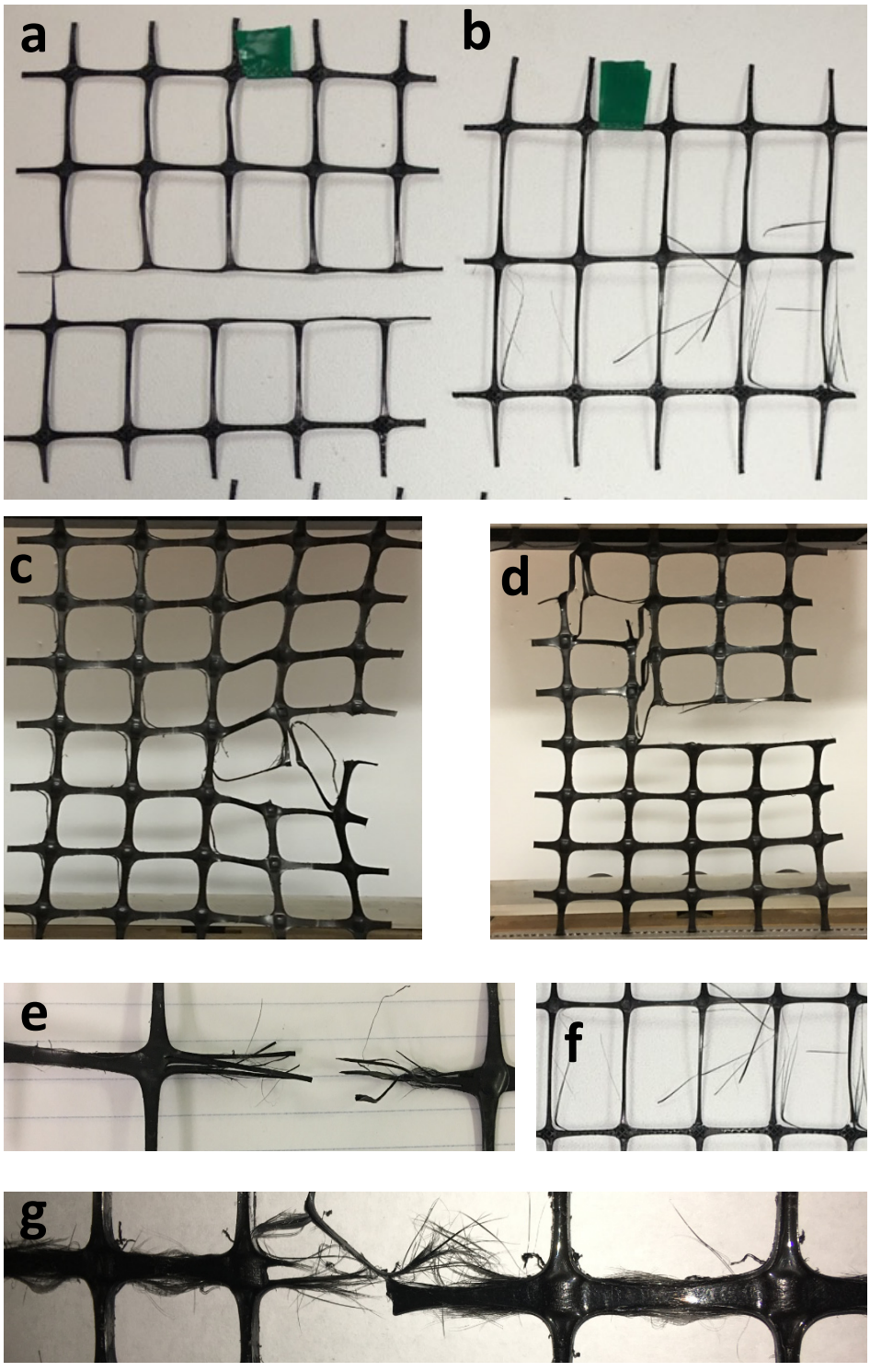

Figure 4.11: Various modes of biaxial geogrid tension failure, a) full failure through ribs and junctions, b) predominant fiber splitting failure, c & d) partial fracture on one side of the specimen through the junctions, e-g) splitting, partial and full fracture of geogrid ribs

4.4 Performance of Uniaxial and Triaxial Geogrids

Results for the geogrids from uniaxial and triaxial geogrids in Figure 4.12 show similar trends compare to the results from biaxial geogrids. Note that for unidirectional geogrids, only the MD was tested in ASTM D6637Method A. The behavior for the triaxial specimens were in line with the biaxial specimens. The uniaxial geogrids tested with Method A show tension strengths comparable with reported values in the literature. Since the failure loads were at much higher levels, the impact of preload is not significant when determining the geogrid properties.

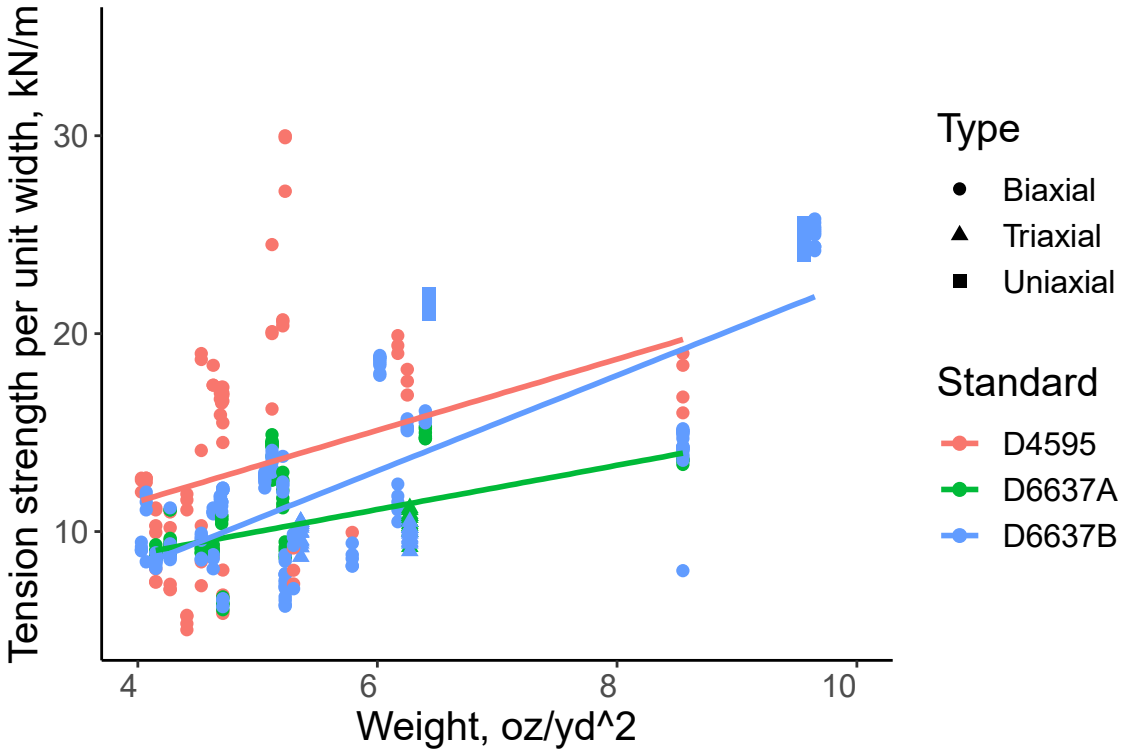

Figure 4.12: Machine direction tension strength per unit width based on 5% elongation

4.5 Proposed Geogrid Tension Strength Specifications

The tension strength laboratory testing program conducted on a significant number of geogrids included various variables such as: (a) majority of manufacturers of geogrid used in WisDOT projects, (b) geogrid types (uniaxial, biaxial, and triaxial), (c) standard testing procedures (ASTM D4595, ASTM D6637 Method A and Method B), and (d) geogrid orientation (machine and cross machine directions). The objective of this research is basically to proposed tension strength specifications for biaxial geogrid acceptance utilizing the results of the testing program. The specifications are based on the ASTM D6637standard procedure.

Statistical analysis was conducted on the biaxial tension strength test results at 5% elongation including Monte Carlo simulation. As shown in Figure 4.13a, the tension strength results at 5% elongation based on the ASTM D4595 standard test procedure exhibited a lognormal distribution. A simulation using 10,000 geogrid tension tests showed consistency between the lognormal distribution (based on the actual test results) and the simulated test results. In addition, the simulation resulted in a cumulative probability plot as in Figure 4.13b in which various percentages of the geogrid tension strength are obtained. For example, 5% of the 10,000 simulated tension tests have tension strength of 487.13 lb/ft (green color in the figure indicates lognormal distribution model), while the tension strength of 481.07 lb/ft is obtained based on the lognormal data (blue color in the figure indicated the 10,000 simulated test results). The simulation is repeated for geogrid test results based on ASTM D6637Methods A & B standard procedure. The results are presented in Figure 4.14. For example, 5% of the 10,000 simulated tension tests have tension strength of 470.43 lb/ft (green color in the figure indicates lognormal distribution model), while the tension strength of 474.57 lb/ft is obtained based on the lognormal data (blue color in the figure indicated the 10,000 simulated test results).

Current WisDOT specifications based on ASTM D4595 standard procedure require geogrid tension strength at 5% elongation to achieve a minimum average of 450 lb/ft for both machine and cross machine direction. Based on the results of the statistical analysis presented in Figures 4.13 and 4.14, 3.6% of geogrid specimens will not pass the current WisDOT tension strength specifications (based on ASTM D6637) and 2.77 % of geogrid specimens will not pass the corresponding tension strength threshold based on ASTM D6637B. Therefore, the research team is proposing an average tension strength minimum of 500 lb/ft for biaxial geogrid in both machine and cross machine directions based on ASTM D6637Method B (multiple ribs). This minimum corresponds to approximately 5% of specimens not achieving such number based on Monte Carlo simulation. It should be noted that the geogrid manufacturers (based on geogrid specifications data sheets published) minimum tension strength tests reported is 550 lb/ft in machine direction and higher numbers for cross machine direction.

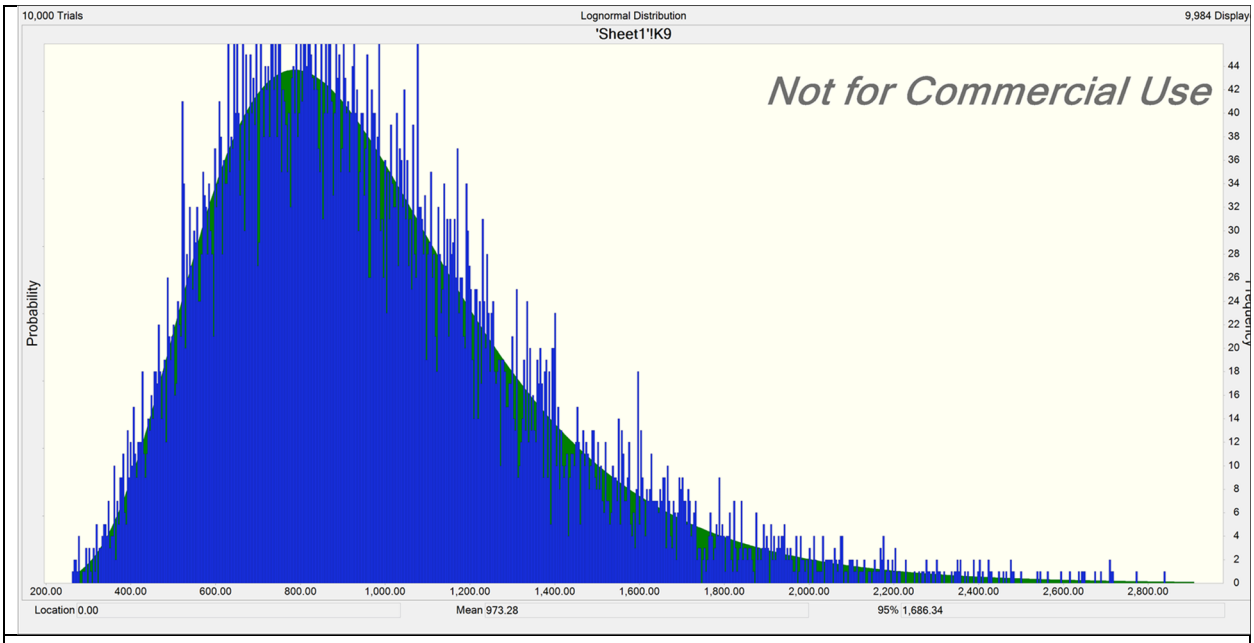

(a) Lognormal distribution versus simulated test results

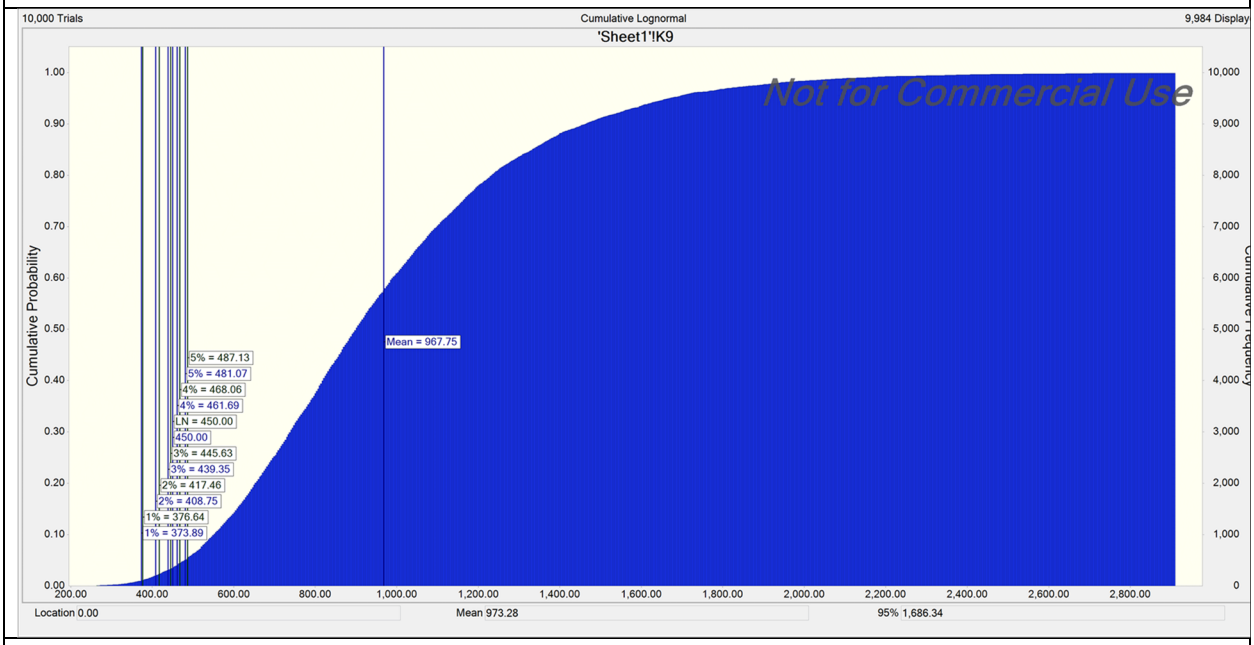

(b) Cumulative probability plot

Figure 4.13: Simulation of tension strength @ 5% strain (using ASTM D4595 in which 10,000 geogrid tests were conducted (Approximately 5% will be <500 lb/ft, based on the test data).

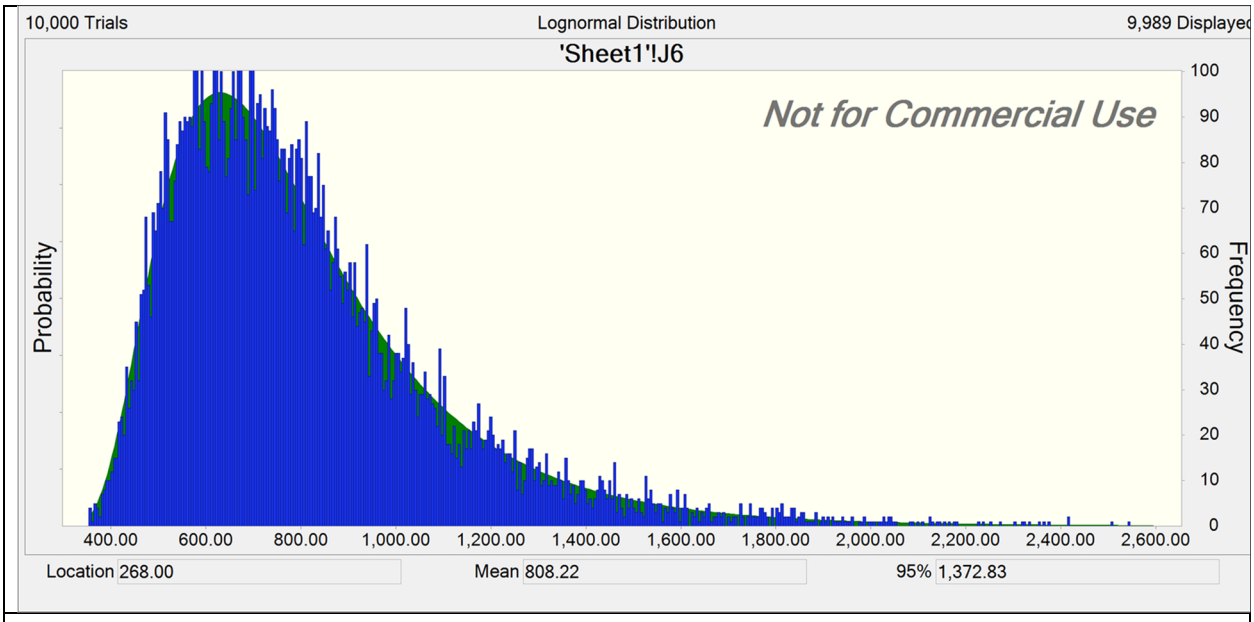

(a) Lognormal distribution versus simulated test results

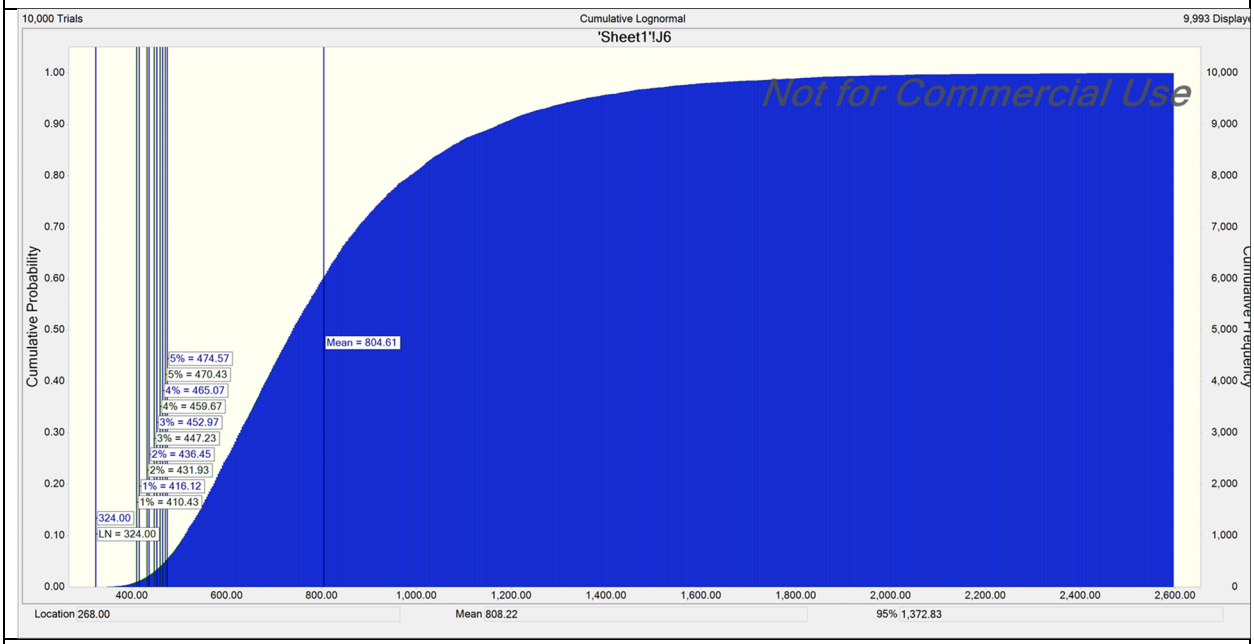

(b) Cumulative probability plot

Figure 4.14: Simulation of tension strength @ 5% strain (using ASTM D6637Methods A & B in which 10,000 geogrid tests were conducted (Approximately 5% will be <500 lb/ft, based on the test data).

4.6 ASTM D4595 versus ASTM D 6637

Under ideal conditions and properties of biaxial geogrid samples subjected to the tension test using ASTM D4596 and D6637, the tensile strength is expected to be of similar values. However, since the wide variability existing in geogrid shape, specimen dimensions, aperture size, and rib thicknesses among other factors such as the human influence there is not a 1:1 correlation between both methods. Based on individual test results and average test results depicted in Figure 4.15, the following average correlation is obtained including both machine and cross-machine direction test results:

$$T_{@5\%}\ (ASTM\ D6637) = 0.921 \times T_{@5\%}\ (ASTM\ D4595) \quad ..... \ R^2 = 0.98$$

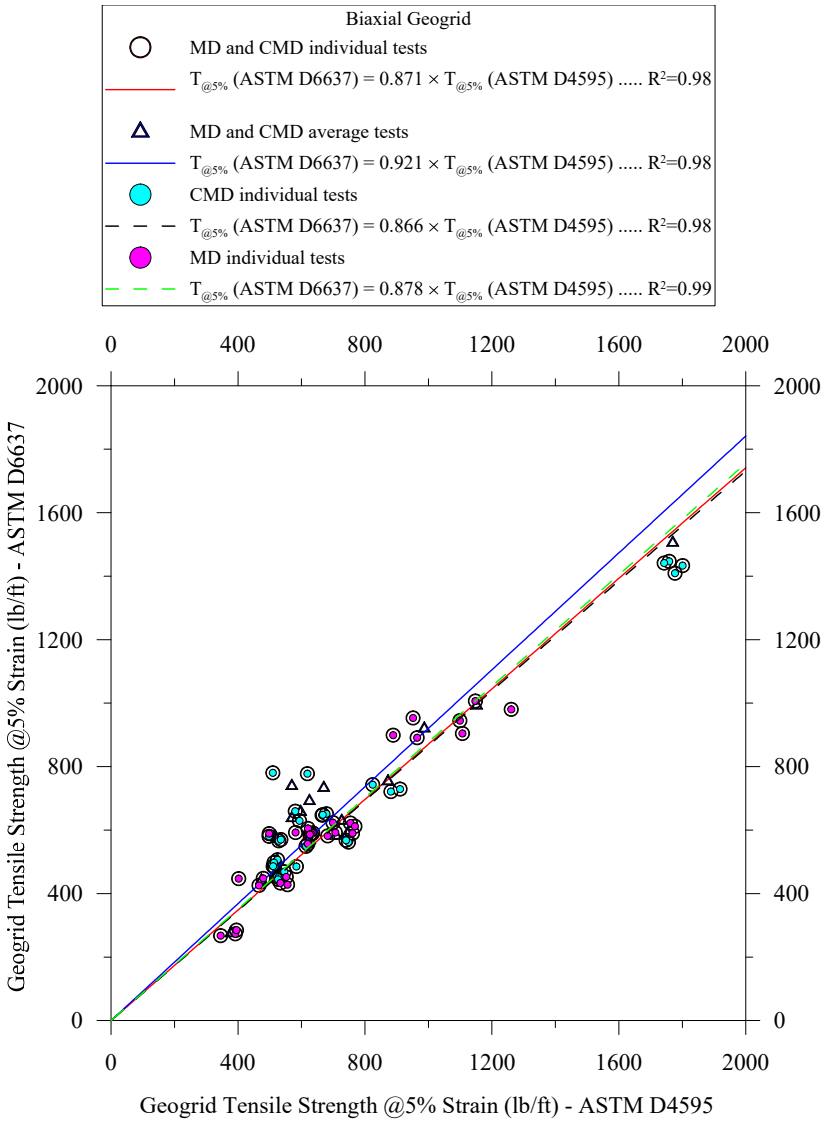

Figure 4.15: Tensile strength of biaxial geogrid @5% strain in both MD and CMD

Chapter 5
Summary, Conclusions, and Recommendations

The Wisconsin Department of Transportation specifications have previously used the ASTM D4595 also known as the "Standard Test Method for Tensile Properties of Geotextiles by the Wide-Width Strip Method," for determining the tension properties of geogrids. The test involves testing an 8-inch wide specimen of the geogrid in the machine and cross machine directions. Strength, elongation and modulus can be measured from his standard. Elongation is measured using cross-head displacement or non-contact extensometers. The gage length is typically 4 inches. A preload of 1% of the breaking force of the material is used before loading the specimen at a constant displacement rate of approximately 10mm/minute to failure. Since ASTM D4595 was originally developed for geotextiles, geogrids have unique differences in geometry which led to the ASTM D6637 standard titled, "Determining Tensile Properties of Geogrids by the Single or Multi-Rib Tensile Method," as the test method most commonly being proposed for assessment of tension properties of geogrids. The standard recognizes that the main factor involving the geogrid tension strength is the ribs per unit length of material versus simply the length. The test standard has three methods, A, B and C. Method A involves determining the tensile properties of a single rib, Method B involves a specimen with multiple ribs and Method C which involves multiple layers. Method B is the most commonly used since it is more representative of the geogrid structure and the load redistribution that may occur in the geogrid in practice. There is also another standard ASTM D7737 titled, "Standard Test Method for Individual Geogrid Junction Strength" which involves testing a single junction in isolation from the ribs. The junction or node is confined such that a single rib is pulled from the junction with the transverse rib used to obtain the maximum force or strength of the junction. Thus, it can be seen that ASTM D6637 derives the tension strength of the ribs of the geogrid whereas ASTM D7737 directly tests the junction of the geogrid. Typically, the junction strength is expected to be within a certain range of the rib strength and maybe an issue especially with the introduction of new materials.

In this project we investigated the application of ASTM D4595, ASTM D6637 and ASTM D7737 on geogrids from more than nine geogrid manufacturers supplying materials for WisDOT projects. The objective was to determine minimum standard guidelines that can be used in practice based on ASTM D6637 and what can be learned from ASTM D7737 on the geogrids used. The choice in geogrid material selection was made to mirror the types of materials, designs and suppliers used on these projects. A total of 987 specimens from biaxial, triaxial and uniaxial geogrids were tested with the bulk of the testing

focused on the biaxial geogrids given they are the most common type. The results show ASTM D6637 resulting in less scatter in the tension strength compared to ASTM D4595 largely due to it more accurately capturing the mechanism of geogrid tension behavior. Variability in machine and cross-machine direction showed importance of testing both directions. While weight of the geogrid can be correlated to the tension strength it is not recommended that the weight be used as a criterion for geogrid material selection to indicate tension strength. Uniaxial and triaxial geogrids were also tested with the standard showing the ability to meet both rib and junction strength requirements for geogrid applications. The strength derived from the 5% elongation was found to yield consistent results and also account for the material nonlinearity before rupture of the specimen. Junction strength from ASTM D7737 showed consistently favorable junction strength compared to rib tension strength ASTM D6637 in all the test specimens examined. In addition, variability in the tension strength of the geogrid roll can be captured by sampling from both edges and the center of the roll.

The results from the junction tests indicate that the rib tests in ASTM D6637 Method B are sufficient for determining the tension strength in the geogrid materials. ASTM D6637 Method B is able to capture the geogrid behavior and account for the variability in the apertures in the roll and the manufacturing or installation related defects.

ASTM D6637 Method A that tests a single rib tracks the results with ASTM D6637 Method B when ultimate strengths are used for a certain range of the geogrid materials. However, when using the loads obtained from the 5% elongation, it is seen that the strain to failure of the two methods do not agree with each other making a direction correlation between Method A and Method B more difficult.

Statistical analysis was conducted on the biaxial tension strength test results at 5% elongation including the use of Monte Carlo simulations. The tension strength results at 5% elongation based on ASTM D4595 and D6637 A and B standard test procedures exhibited a lognormal distribution. A simulation using 10,000 geogrid tension tests showed consistency between the lognormal distribution (based on the actual test results) and the simulated test results for both standard test procedures.

Current WisDOT specifications based on ASTM D4595 standard procedure require geogrid tension strength at 5% elongation to achieve a minimum average of 450 lb/ft for both machine and cross machine direction. Based on the results of the statistical analysis, 3.6% of geogrid specimens will not pass the current WisDOT tension strength specifications (based on ASTM D4595). It also lacks the ability to capture the material variability in the roll, because of the lack of any corrections for that effect.

The research team based on the comprehensive laboratory testing program and corresponding analysis concludes that ASTM D6637 more accurately and consistently represents the tension strength of

geogrid materials with less variability and more accurately across the roll than ASTM D4595. The research team recommends an average minimum tension strength of ***500 lb/ft for biaxial geogrid in both machine and cross machine directions*** based on ASTM D6637 Method B (multiple ribs) for accepting geogrid in WisDOT projects for subgrade improvement/stabilization and base reinforcement. This minimum corresponds to approximately 5% of specimens not achieving such number based on Monte Carlo simulation when using the data set generated. It should be noted that the geogrid manufacturers (based on published geogrid specification data sheets) report the minimum tensile strength is 550 lb/ft in the machine direction and typically higher numbers for cross machine direction strength for common geogrids used on WisDOT projects and studied in this report.

References

Ahmadi, M. S. and P. N. Moghadam (2017). "Effect of Geogrid Aperture Size and Soil Particle Size on Geogrid-Soil Interaction under Pull-Out Loading." Interaction **13**: 16.

ASTM D4595 'Standard Test Method for Tensile Properties of Geotextiles by the Wide-Width Strip Method. West Conshohocken, PA.

ASTM D6637 'Standard Test Method for Determining Tensile Properties of Geogrids by the Single or Multi-Rib Tensile Method'. West Conshohocken, PA.

ASTM (2015). "ASTM D6637 / D6637M - 15 - Standard Test Method for Determining Tensile Properties of Geogrids by the Single or Multi-Rib Tensile Method, ASTM International,West Conshohocken, PA."

ASTM (2016). "ASTM D5262-07(2016) - Standard Test Method for Evaluating the Unconfined Tension Creep and Creep Rupture Behavior of Geosynthetics, ASTM International, West Conshohocken, PA, 2016."

Bathurst, R. J. and Y. Miyata (2015). "Reliability-based analysis of combined installation damage and creep for the tensile rupture limit state of geogrid reinforcement in Japan." Soils and Foundations **55**(2): 437-446.

Berg, R. R. and R. Bonaparte (1993). "Long-term allowable tensile stresses for polyethylene geomembranes." Geotextiles and Geomembranes **12**(4): 287-306.

Cardile, G., N. Moraci and M. Pisano (2016). "Tensile behaviour of an HDPE geogrid under cyclic loading: experimental results and empirical modelling." Geosynthetics International **24**(1): 95-112.

Carrol Jr, R. (1988). "Specifying geogrids." Geotechnical Fabrics Report **6**(2).

Dong, Y., J. Han and X. Bai (2010). A numerical study on stress-strain responses of biaxial geogrids under tension at different directions. GeoFlorida 2010: Advances in Analysis, Modeling & Design**:** 2551-2560.

Dong, Y.-l., H.-j. Guo, J. Han and J. Zhang (2018). "Numerical analysis of installation damage of a pre-damaged geogrid with rectangular apertures." Results in Physics **9**: 1185-1191.

Dong, Y.-L., J. Han and X.-H. Bai (2011). "Numerical analysis of tensile behavior of geogrids with rectangular and triangular apertures." Geotextiles and Geomembranes **29**(2): 83-91.

França, F., F. Avesani, B. Bueno and J. Zornberg (2013). "Confined-accelerated creep tests on geosynthetics." Proceedings. Geosynthetics 2013.

França, F., B. Bueno and J. Zornberg (2012). New equipment to conduct confined-accelerated creep tests on geosynthetics. 14th Pan-American Conference on Soil Mechanics and Geotechnical Engineering.

Franca, F., B. Massimino, J. Silva, F. Iceri and J. Zornberg (2014). Geogrid creep and tensile tests performed with nonconventional equipment. Proceedings of the 10th International Conference on Geosynthetics, 10ICG, Berlin, Germany.

Hegazy, R., G. M. Mahmoud and E. H. Hasan (2018). "Effect of Strain Rate on Tensile Testing of Geogrid Reinforcements Using Single-Rib and Wide-Rib Specimen." Advances in Polymer Technology **37**(4): 1185-1192.

Hsieh, C.-W. and Y.-C. Tseng (2008). "Tensile creep behavior of a PVC coated polyester geogrid at different temperatures." Journal of GeoEngineering **3**(3): 113-119.

Hsieh, C. W. (2009). Tensile and Creep Behavior of Polyvinyl Chloride-Coated Polyester Geogrid at Different Temperatures. https://trid.trb.org/view/881051.

Hsieh, C. W. and C.-K. Lin (2004). "Tensile test method effect on the tensile strength of flexible PET geogrids." Geotechnical Testing Journal **27**(1): 111-118.

Institute, G. R. (1987). GRI Test Method GG1-87_Geogrid Rib Tensile Strength. Drexel University, Philadelphia.

Institute, G. R. (1987). GRI Test Method GG2-87_Geogrid Junction Strength. Drexel University, Philadelphia.

ISO, E. (2015). "10319:2015 Geosynthetics- Wide-Width tensile test."

Jeon, H. Y., S. H. Kim and H. K. Yoo (2002). "Assessment of long-term performances of polyester geogrids by accelerated creep test." Polymer Testing **21**(5): 489-495.

Ji-ru, Z., X. Lin and L. Zhe-an (2002). "Material properties and tensile behaviors of polypropylene geogrid and geonet for reinforcement of soil structures." Journal of Wuhan University of Technology-Mater. Sci. Ed. **17**(3): 83-86.

Kaliakin, V. and M. Dechasakulsom (2001). Time-Dependent Behavior of Geosynthetic Reinforcement–A Review of Experimental Work, Citeseer.

Kongkitkul, W., Tabsombut, W., Jaturapitakkul, C., & Tatsuoka, F. (2012). Effects of temperature on the rupture strength and elastic stiffness of geogrids. *Geosynthetics international*, *19*(2), 106-123.

Khillari, S. (2020). "Geosynthetics Market| Growth, Trends and Forecast Report, 2026."

Kim, J. H., Y.-H. Byun, I. I. Qamhia, M. F. Orihuela, E. Tutumluer and M. Wayne (2019). Investigation of Aggregate Particle and Geogrid Aperture Sizes for Mechanical Stabilization Using Bender Element Shear Wave Transducers.

Kupec, J. and A. McGown (2004). The Biaxial load-strain behaviour of Biaxial Geogrids. Proceedings of the 3rd Asian Regional Conf. on Geosynthetics, Citeseer.

Kupec, J., A. McGown and A. Ruiken (2004). Index testing of the junction strength of geogrids. Proc. of the 3rd Asian Regional Conf. on Geosynthetics Now and Future of Geosynthetics in Civil Engineering (Seoul).

Leshchinsky, D., M. Dechasakulsom, V. Kaliakin and H. Ling (1997). "Creep and stress relaxation of geogrids." Geosynthetics International **4**(5): 463-479.

McGown, A., J. Kupec, G. Heerten and K. Von Maubeuge (2005). Testing biaxial geogrids for specification and design purposes. Geosynthetics Research and Development in Progress**:** 1-11.

Nicola, M. and M. Filippo (1997). Behavior of geogrids under cyclic loads.

Qian, Y., J. Han, S. Pokharel and R. Parsons (2011). "Stress Analysis on Triangular-Aperture Geogrid-Reinforced Bases over Weak Subgrade Under Cyclic Loading." **2204**: 83-91.

Qian, Y., J. Han, S. K. Pokharel and R. L. Parsons (2012). "Performance of triangular aperture geogrid-reinforced base courses over weak subgrade under cyclic loading." Journal of Materials in Civil Engineering **25**(8): 1013-1021.

Sawicki, A. (1998). "A basis for modelling creep and stress relaxation behaviour of geogrids." Geosynthetics international **5**(6): 637-645.

Shinoda, M. and R. J. Bathurst (2004). "Lateral and axial deformation of PP, HDPE and PET geogrids under tensile load." Geotextiles and Geomembranes **22**(4): 205-222.

Shrestha, S. and J. Bell (1982). A wide strip tensile test of geotextiles. Proceedings of the Second International Conference on Geotextiles, IFIA Las Vegas.

Shukla, S. K. (2002). Geosynthetics and their applications, Thomas Telford.

Sissons, C. (1977). Strength testing of fabrics for use in civil engineering. International Conference on the Use of fabrics in Geotechnics.

Stevenson, P. E. (2000). Grips, clamps, clamping techniques, and strain measurement for testing of geosynthetics, ASTM.

Tang, X., G. R. Chehab and A. Palomino (2008). "Evaluation of geogrids for stabilising weak pavement subgrade." International Journal of Pavement Engineering **9**(6): 413-429.

Whelton, W. and N. Wrigley (1987). Long-term durability of geosynthetics soil reinforcement. Proceedings of Geosynthetic'87 Conference, New Orleans, LA.

Yang, G.-q., W. Pang, L. Peng and Q.-y. Zhou (2008). "Experimental study of tensile properties of geogrids [J]." Rock and Soil Mechanics **9**.

Yeo, S. S. and Y. G. Hsuan (2010). "Evaluation of creep behavior of high density polyethylene and polyethylene-terephthalate geogrids." Geotextiles and Geomembranes **28**(5): 409-421.

Yoo, C.-S., H.-Y. Jeon and S.-B. Kim (2008). "Time-dependent Deformation Charateristics of Geogrid Using Wide Width Tensile Test." Journal of the Korean Geotechnical Society **24**(1): 71-80.

Zanzinger, H., H. Hangen and D. Alexiew (2010). "Fatigue behaviour of a PET-Geogrid under cyclic loading." Geotextiles and Geomembranes **28**(3): 251-261.

Zheng, C., J. Liu, J. Fan, Y. Luan and L. Song (2016). "Research on deformation behavior of isotactic polypropylene in uniaxial geogrid manufacture." Materials & Design **91**: 1-10.

Zhuang, Y. and K. Wang (2015). "Three-dimensional behavior of biaxial geogrid in a piled embankment: numerical investigation." Canadian Geotechnical Journal **52**(10): 1629-1635.